

Design, simulation and testing of novel compact and robust geared powertrain

Zhaksylyk Galym, bachelor's in mechanical engineering

**Submitted in fulfillment of the requirements
for the degree of Master of Science
in Mechanical & Aerospace Engineering**



**School of Engineering and Digital Sciences
Department of Mechanical & Aerospace Engineering
Nazarbayev University**

53 Kabanbay Batyr Avenue,
Nur-sultan, Kazakhstan, 010000

Supervisors: Professor Christos Spitas
Professor Konstantinos Kostas

April 2020

Acknowledgments

I would like to express my gratitude towards my supervisors Christos Spitas and Konstantinos Kostas. It has been their supervision and direction throughout my studies which have allowed me to complete this Master's program. I am appreciative for their support throughout the working process and for all the hours of discussion they have offered me.

Abstract

Common issues of geared powertrain systems are discussed in this work such as gear misalignment in conventional gearboxes and reliability issues of typical planetary gears. An extensive literature review was performed for each topic. For the misalignment issue, multiple solutions were proposed including misalignment insensitive gearing integrated with Rzeppa or constant velocity ball joint and spur gears with the modified web with thin flexible rim topology. All proposed models, and a benchmark model in the form of regular spur gears and flank modified gears were compared in terms of misalignment insensitivity. According to results, a novel gears with kinematical joint display the most superior performance in terms of gear mesh stress, with the compromise being increased stress results in internal interfaces. On the other hand, compliant web gears show moderate effectiveness against the issue and flank modification could mitigate misalignment to some extent. In terms of transmission error (TE), the gear with the Rzeppa joint demonstrates complete insensitivity to misalignment, despite experiencing high TE, whereas the conventional gears suffer from misalignment significantly, with TE amplitude increasing rapidly as misalignment angle becomes bigger.

For the case of planetary gears, a planetary gearbox with novel topology and the floating carrier was presented. The key feature of the design was the elimination of bearing interface existing in the generic layout of the planetary gear set. Bearings of planets' carriers tend to fail frequently, leading to misalignment and vibrations. The novel planetary gears were simulated using FEA and MBD to evaluate the viability of the concept. Despite replacing the bearing contact with robust geared connection, simulations results show that the novel bearingless planetary gearbox with floating carrier still suffers from common issues such as non-equal load distribution and misalignment.

Table of contents

Abstract	4
List of Abbreviations & Symbols	6
List of figures	8
Chapter 1 – Introduction	9
1.1 General	9
1.2 Problem statement and hypothesis	11
1.3 Objective of the thesis	12
1.4 Scope of work	12
Chapter 2 – Misalignment-insensitive gearing using kinematic Rzeppa joint and various compliant web designs	12
2.1 Literature review	12
2.2 3D Modelling	16
2.3 Numerical modeling	20
2.4 Meshing	22
2.5 Transmission error (TE) calculation.....	29
2.6. Results and discussion	29
2.6.1. Benchmark model (Model A)	29
2.6.2. Crowned gears (Model B).....	30
2.6.3. Proposed design (Model C)	30
2.6.4. Gear with compliant web (Model D and Model E)	31
Chapter 3 – Bearingless floating-carrier compound planetary gearbox	36
3.1 Literature review	36
3.2. 3D Modelling	40
3.3. Numerical modeling	42
3.5. Results and discussion	46
Chapter 4 – Conclusion.....	49
Bibliography	51

List of Abbreviations & Symbols

FEA	Finite Element Analysis
FEM	Finite Element Methods
MBD	Multi-body dynamics
CAE	Computer-Aided Engineering
TE	Transmission error
α	Angle of misalignment
α_0	Pressure angle
z_1	Number of teeth of the gear
z_2	Number of teeth of the pinion
θ_1	The angular position of the gear
θ_2	The angular position of the pinion
C	Crowning magnitude
w	Tooth width
m	Normal module
a	Center
N	Number of elements (in thousands)
σ	Contact stress
σ_0	Contact stress of non-misaligned non-modified spur gears
σ_{ref}	Reference stress
k	Stiffness coefficient
c	Damping coefficient
m1	Stiffness exponent
m2	Damping exponent
m3	Indentation exponent
δ	Penetration
$\dot{\delta}$	Time differentiation of penetration

f_n

Normal force

f_f

Friction force

List of figures

Figure 2. 1 Thin rimmed spur gears with inclined webs at the left, center and right side of the tooth (Li, 2012)	16
Figure 2. 2. 3D gear pair generated in KissSoft	17
Figure 2. 3. Crowning parameters	17
Figure 2. 4. Proposed design with Rzeppa-type joint.....	19
Figure 2. 5 Thin rimmed gear with inclined web	19
Figure 2. 6 Geometric model of misaligned gears (α is the misalignment angle)	20
Figure 2. 7 Main components of the simplified design used in this study	21
Figure 2. 8 Boundary conditions of the benchmark and crowned system.....	22
Figure 2. 9 Boundary conditions of the proposed design	22
Figure 2. 10 Location of the reference points	23
Figure 2. 11 Meshing along the tooth mesh contact (Point X)	24
Figure 2. 12 Meshing of groove-ball interference (Point Y)	25
Figure 2. 13 Meshing of tooth mesh contact line (Point Z).....	25
Figure 2. 14 Meshing of tooth mesh contact line (Point T).....	26
Figure 2. 15 Mesh sensitivity analysis.....	26
Figure 2. 16 Mesh elements of the benchmark design	27
Figure 2. 17 Mesh elements of the proposed design	27
Figure 2. 18 Mesh elements of the crowned design.....	28
Figure 2. 19 Mesh elements of the web modified design	28
Figure 2. 20 Contact stresses for benchmark design (Model A) for different misalignment values	30
Figure 2. 21 Contact stresses of crowned design (Model B, crowned) for different misalignment values	30
Figure 2. 22 Proposed design (Model C) at any misalignment.....	31
Figure 2. 23 Vector displacement field, showing the automatic realignment action of the proposed design.....	31
Figure 2. 24 Gear with compliant web with 0.2mm thickness (Model D)	32
Figure 2. 25 Gear with compliant web with 0.4mm thickness (Model E).....	32
Figure 2. 26 Deflection of thin compliant rim	32
Figure 2. 27 Non-dimensional stress plot along the contact line for various designs.	34
Figure 2. 28 Static TE.....	35
Figure 3. 1 The circuit diagram of the proposed gear.	40
Figure 3. 2 3D model of bearingless planetary gear with floating carrier	41
Figure 3. 3 Misalignment preventing raceways	42
Figure 3.4 Simplified model of the planetary gear for quasi-static FEA	43
Figure 3.5 Boundary conditions for the planetary gear	43
Figure 3.6 Discretized model the planetary gear	44
Figure 3.7 MBD simulation setup for the bearingless planetary gearbox	46
Figure 3. 8 FEA results of bearingless planetary gearbox with floating carrier	47
Figure 3. 9 Deformation results of the novel planetary gears	48
Figure 3. 10 Input and output velocity graphs	49

Chapter 1 – Introduction

1.1 General

The powertrain is an important part of any machinery whose main purpose is to deliver a power generated by an engine or motor to the desired point in form of rotational, reciprocal, translational, etc. movements. Also, robustness, reliability, and compactness of powertrains are primary interests, considering current trends in design engineering. The most common object in most powertrain systems is gearing transmissions or geared connections. Ideally, the power transmission through geared connections should be reliable, efficient, smooth and as much as possible free from excessive loads (e.g. at the tooth interface) and/ or Transmission Errors (TE). However, in the case of real-life, different gear problems such as impact fracture, fatigue, wear, and stress rupture is inevitable, with gear fatigue being the most frequent reason of gearbox failure. In general, gearboxes are found to be one of the most reliable and durable mechanical devices. Despite this fact, gearboxes suffer from various reliability issues, mostly caused by application errors. Application errors are improper maintenance, vibrations, installation errors, and thermal stresses. However, the most common and severe application error in geared transmissions is misalignment (Asi, 2006). In case of misalignment, due to the abnormal meshing between pinion and gear, the stress concentration region appears along the contact surfaces. Moreover, improper alignment causes excessive heat generation and wear of contacting surfaces. For example, in gears, micro-pitting starts occurring in the stress concentration areas. Some factors inducing gear misalignment are manufacturing and installation errors, which are static causes, whereas deflection of shafts due to excessive load and thermal expansions are dynamic causes. Currently, the most well-known solution to gear misalignment is a flank modification or crowning. To reduce detrimental effects of the alignment error, gear material is removed from tooth surface eliminating corners, resulting in the curved tooth surface. Apart from, only partially removing the negative impacts of misalignment, crowning demands expensive machining with high accuracy (Neha & Shunmugam, 2017). Thus, the flank modification cannot fully solve the gear misalignment problem, and new solutions are required.

Planetary gears have found their applications in different fields of engineering, especially in automotive, robotics, and aerospace industries. Comparing with conventional mechanical transmission systems, planetary gear transmissions are decently compact and provide a larger transmission ratio with high efficiency. Automatic car gearboxes are the best

example of it. Planetary gear drive is the mechanism or transmission with more than one degree of freedom that gives the desired output for the given input (e.g. torque) (Chaari et al., 2005). Such a gear drive system got its name due to its similarity to the motion of the solar planetary system, where planets go around the sun in a fixed trajectory. A standard planetary gear drive consists of the sun gear in the center, which drives the planetary gears in fixed internal gear also known as the ring gear, and the output is given by the carrier. Alternatively, the fixed-gear might be chosen to be sun gear or the carrier with the planet gears, and consequently, the output variable will be changed respectively (del Castillo 2002). Ideally, within planetary gears loads should be equally distributed between planets, which makes such mechanisms highly attractive for high power density applications. However, in real-life applications, this load distribution is not equal causing an increase in bearing forces, which in turn, leads to early bearing failure. Thus, the load sharing capability is a crucial parameter for the gearbox reliability (Guo, Keller & LaCava, 2012). Also, based on statistics, in the renewable energy sector, 30% of gearbox failures are caused by gearbox bearing or planetary stage damage caused by unequal load sharing. On the other hand, during the gearbox designing stage, clearance of planetary gear bearings takes into account surface tolerance and possible thermal expansion. However, these clearances cause the planetary stage to misalign, which in turn increases vibrations and leads to unequal load allocation within individual planets (Gu & Velez, 2013). Therefore, it is important to develop a planetary gearbox for high-speed applications with a novel topology which is insensitive to inherent problems of typical planetary gearboxes.

Considering reliability issues, the main purpose of this thesis work is to develop, design and investigate numerically robust and compact powertrains with geared transmissions. Particularly, this paper focuses on dealing with misalignment issues in geared transmissions and proposes multiple solutions to the problem. The proposed alternatives will be compared with the existing solutions as well. In addition, the paper considers developing and suggesting a planetary gear transmission with novel topology, with replaced carrier bearing. Since the existing work consists of two main parts, each topic, including respective extensive literature reviews, is written separately and they are arranged in the following way:

Chapter #1: Misalignment-insensitive gearing using kinematic Rzeppa joint and various compliant web designs

Chapter #2: Bearingless floating-carrier compound planetary gearbox

1.2 Problem statement and hypothesis

Due to increasing quality reasons, errors in the geometry and alignment issues must be stayed away in machinery and this is the reason why progressively stringent tolerances and correspondingly accurate assembling and manufacturing are being applied to gears utilized in aviation, automotive industry, and energy generation. However, despite significant development in manufacturing and production approaches, there is still some inevitable compromise between low cost and high-quality manufacturing, as well as weight reduction and stiffness loss. Gear manufacturing and gearbox production is not an exception. It is impossible to have perfect alignment between individual parts. As a result, these factors lead to improper alignment of gears, which in turn causes undesired vibrations and abnormal noise emission, as well as premature failure due to uneven stress distribution along the primary tooth contact line (Ameen, 2010).

In addition, an existing solution for gear misalignment such as crowning is not capable to fully mitigate adverse effects on the alignment issue. Also, flank modification is costly and requires high accuracy manufacturing. Therefore, there is a need for an effective solution against the aforementioned problem. Constant velocity ball joints or kinematical joints or Rzeppa joints are typically used by car manufacturing, especially in front-wheel drives. These universal joints have long been used to deliver a torque between two arbitrary located shafts at different misalignment angles. By integrating this mechanical device with the regular spur gears, this paper hypothesizes that the application of the kinematical joint could solve the misalignment issue in gearboxes.

Planetary gearboxes offer some exceptional characteristics such as high efficiency and decent load carrying capacity with large power density. These characteristics made planetary gearboxes attractive to different fields. However, planetary gearboxes tend to fail frequently because of unequal load sharing caused by bearing failure and planets misalignment, which decreases reliability. Therefore, it could be concluded that designing a new generation robust model of planetary gears could solve some of the powertrain issues that industries are struggling with. As will be discussed in the extensive literature review, in the case of traditional planetary gearboxes gear misalignment and bearing failures are responsible for the majority of reliability issues. For instance, increased bearing clearance leads to premature resonance state of the system and failure of individual components. Therefore, this paper proposes a novel design of a bearingless floating-carrier compound planetary gearbox, and hypothesize that it helps to get rid of inherent drawbacks of the generic model, and considers elimination of bearing contact

from the traditional design by replacing it with more robust gearing contact. In addition, a unique leading groove with a triangular feature enables better alignment of individual gear components, ensuring stable operation. Apart from the removed bearing components and newly introduced grooves, the proposed model inherits the superior attributes of the conventional planetary gear such as large transmission ratio, high power density, and compactness.

1.3 Objective of the thesis

First, this thesis work aims to propose, design, evaluate and compare different concepts of misalignment insensitive gear transmission with compliant web and kinematical joint for powertrain applications. Evaluation of the viability of the concepts is performed by means of different CAE tools. The main objective of the second subtopic is to propose a new model bearingless planetary gear with a floating carrier which can be used in high-speed applications. The proposed model of the gearbox system will be analyzed using FEA to estimate loads and deformations. Dynamical simulations will be performed in MBD software as well.

1.4 Scope of work

This work considers modeling and simulation of multiple geared transmissions. In the case of the misalignment gearing, regular spur gears will be compared against the flank modified model, as well as proposed designs with Rzeppa joint and thin web structure, in terms of misalignment insensitivity. All models will be evaluated for load-carrying capability, stress distribution in non-misaligned and in-plane angular misaligned cases. In the bearingless floating-carrier compound planetary gearbox, the dynamics, load-carrying capabilities of the novel design will be assessed by means of FEA and MBD software.

Chapter 2 – Misalignment-insensitive gearing using kinematic Rzeppa joint and various compliant web designs

2.1 Literature review

There is a big amount of literature dedicated to studying misalignment in gears and its nature. Gear misalignment is mostly caused by improper alignment of gear carrying shafts. Linear and angular misalignments are found to be two main categories of gear alignment error

and both types negatively influence gear contact and meshing (Hu and Mao, 2017). Moreover, Hu and Mao (2017) went beyond and reported four distinguishable gear misalignment types such as axial, radial, yaw and pitch subtypes. Axial and radial misalignments belong to the linear category, while yaw and pitch are found to be angular. In addition, radial – e.g. deviations in the center distance (Amani, 2015), along with axial and yaw misalignments are in-plane misalignments, whilst pitch misalignment is out of plane.

Experiment results on spur gears made of plastic at different misalignment conditions showed that the contact area exhibited extreme sensitivity to angular misalignments, rather than linear misalignments. Kumar et al. (2018) moved further in analyzing the effective contact area between a pair of misaligned gears. According to the authors, the contact area between two gears diminishes significantly in the case of angular misalignments compared to linear misalignments. They found out experimentally, that in case of angular misalignment the originally quadrilateral shape of the effective contact area becomes triangular. Additional to the contact area reduction, improper alignment degrades the mechanical properties of the geared transmission. By experimentally comparing the contacts in misaligned and non-misaligned scenarios, Glodez et al. (1998) concluded that in a one-sided load distribution condition, gears tend to fracture prematurely, whereas evenly distributed load conditions provide maximum fatigue life of the geared transmissions. Saxena et al. (2014) studied the effects of shaft misalignment and friction between meshing tooth pairs on the time-varying mesh stiffness of spur gears and showed that gear alignment error leads to increased vibrations in the gear pair. Indeed, this is consistent with the later findings by Neha and Shunmugam (2017), as there is a well-established dependency between time-varying mesh stiffness and transmission error. Moreover, gear misalignment was shown to decrease gear stiffness several times. Eng et al. (2018) established an empirical relation between the maximum contact stress and axial and angular misalignments for frictionless and frictional scenarios. They found out that the introduction of frictional behavior to the contact area between misaligned gears leads to a noticeable increase in maximum contact stress and bending stress at the tooth root. In addition, several researchers developed analytical approaches to estimate the bending stress at the tooth root and the maximum stress along the contact line: E.g. Sánchez et al. (2016) derived new methods of calculating of loading conditions of spur gear teeth, which were based on the new model of load distribution, by taking into account derivation in rigidity factor along the contact line. Various more scientific papers have dealt with the topic of gear misalignment in past years by implementing different approaches. Several researchers such as Jammal et al. (2015),

Shubham et al. (2016) and Seol and Kim (1998) investigated spur gears and by means of FEA carried out dynamic and static simulations. They revealed that results obtained synthetically are in good agreement with experimental and analytical solutions, which are based on Hertzian stress theory and Lewis' equations, thus proving the applicability of Finite Element simulations to the problem.

In recent decades, several solutions for gear misalignment were proposed by various researchers. Mao (2006) examined tooth profile modification and its impact on misalignment stress reduction in different gears, reporting that tooth modifications such as crowning are able to significantly decrease stress concentration at the contact area. Mao also noted that coating the gear tooth surface by tungsten alloys is able to strengthen the gear against the overloads induced by the alignment error; however, he concluded that the approach is not an adequate solution to the issue. Ye and Tsai (2015) in their investigation of High Contact Ratio (HCR) gears under different conditions of gear shaft misalignment, tooth deformation and tooth profile modifications showed that angular misalignment causes the maximum stress to increase significantly. While tooth flank modification (crowning) caused the misalignment sensitivity to become less, average stress values between meshing teeth were increased due to the localization of tooth contact and the reduction of the contact area compared to the nominal design. In addition, Neha and Shunmugam (2017) confirmed these findings in an independent investigation of spur gear pairs with and without flank modification under different alignment conditions. Simulation results showed that in case of alignment error conventional unmodified gears suffer from excessive stress values, in addition to the introduction of transmission error. They furthermore showed that introducing crowning leads to a reduction of these abnormal stress values, and mitigates the effects of misalignment to some extent, but at the cost of increased vulnerability to micro-pitting because of the reduction of the contact area. Apart from the aforementioned works, Pop and Cretu (2017) studied the effect of crowning on the lead profile, which is used to mitigate the appearance of the edge effect. To investigate the area of contact, allocation of pressure and states of depth stress of the simple and crowned gears a semi-analytical technique was utilized. The modification of the profile was based on the crowning of the end relief of the tooth flanks and the flank surface. As reported by authors, spur gears with longitudinally crowned flank profiles produce a relatively smooth pressure distribution and avoid the edge effect, which makes them a competent solution for gear misalignment. Li (2015) also examined gear misalignment and suggested tooth flank modification as an effective remedy. Furthermore, he stated the importance of finding optimal crowning parameters based

on loading conditions and misalignment amount. Optimal tooth profile modification reduces the risk of micro-pitting in crowned gears.

Nonetheless, in spite of several researchers proposing tooth modification or crowning as an effective solution against the detrimental effects of gear misalignment, there are disadvantages related to the technology. Even though experimental works conducted by Hotait and Kahraman (2008) on a misaligned crowned gear pair proved the efficacy of the tooth shape modification, supporting above-mentioned authors, they also mentioned the significant increase in maximum root and contact stresses caused by the considerable reduction of the contact area, meaning premature failure might occur. Moreover, excessive tooth flank modification causes vulnerability to micro-cracks and micro-pitting, decreases the overall durability of a gear tooth and can actually worsen dynamical response (Spitas, 2006), while too small crowning poses problems for bearing contact stability (Seol and Kim, 1998). In addition, introducing crowning to a gear pair requires an additional manufacturing step. According to Young (2010), gear tooth crowning consists of two stages: roughing and shaving. Roughing or pure crowning does not give sufficient tooth surface finish, hence followed by shaving technique, which removes burrs and tooth surface irregularities by the high-precision grinding process. Therefore, tooth flank modification consists of time-consuming processes, requires high-precision machining and additional investment.

Apart from tooth flank modification, there are some promising solutions for gear alignment problems. Barbato et al. (2016) developed a mathematical model of a system to monitor and correct angular and linear misalignment of gears in real-time. The novel technology then tested to realign automatically gear pair by integrating various positioning sensors. The automatic gear aligning system led to a reasonable reduction in gear aligning time provided much more precise positioning, but this solution is highly dependent on the accuracy of sensors and, due to its requirement of a relatively complex active system, is not cost-effective. Another interesting solution to the misalignment problem was introduced and analyzed by Li (2012): Thin rimmed spur gears with inclined webs at the left, center and right side of the tooth were analyzed in this study using FE methods combined with a mathematical programming method (Figure 2.1).

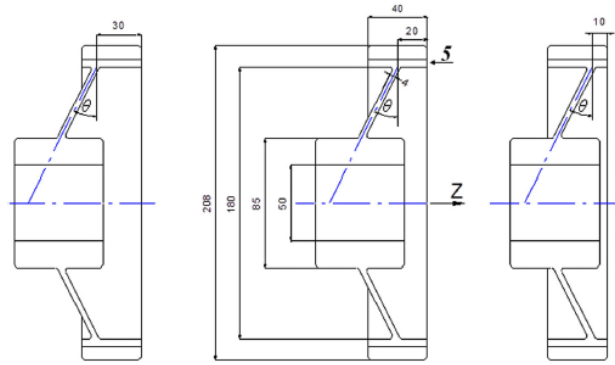


Figure 2. 1 Thin rimmed spur gears with inclined webs at the left, center and right side of the tooth (Li, 2012)

The study showed that altering gear web by making thin-rimmed gears have a significant influence on the stresses, in some cases leading to a reduction in stresses.

2.2 3D Modelling

The study considers five design models, named A-E:

- A. A benchmark geometry, which is a pair of regular spur gears without any improvements nor modifications,
- B. A flank-modified design with a crowning
- C. Proposed design with kinematical joint topology (without crowning)
- D. Proposed spur gears with the modified thin compliant web with a thickness of 0.2mm
- E. Proposed spur gears with the modified thin compliant web with a thickness of 0.4mm

A spur gear pair with a kinematical joint and offered designs with compliant web are the main focus of the work. To allow a generalization of the results, a non-dimensional approach was implemented (Amani, Spitas, & Spitas, 2017) where all length magnitudes were expressed in relation to the module. Geometrically precise models of the spur gear and pinion of the system (including crowning, where applicable) were constructed on the KissSoft platform, using the following non-dimensional parameters: $m=5.5$, $\alpha_o = 20^\circ$, $z_1=25$, $z_2=15$, $a=20$ (nominal), $w=6.2$ (nominal) (Figure 2.2).

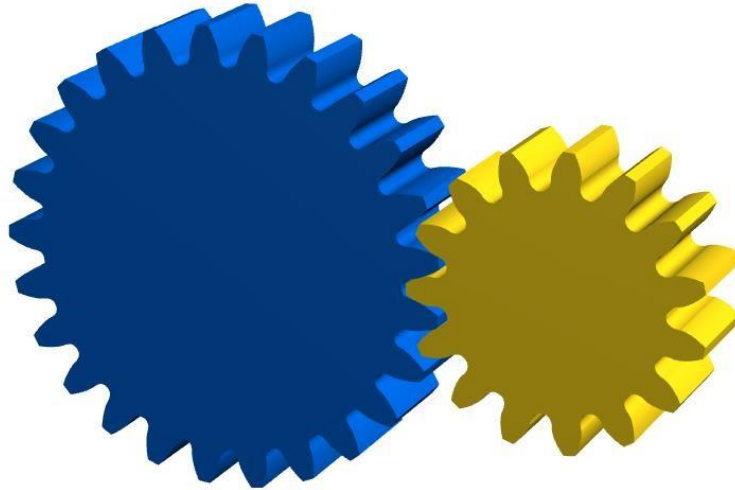


Figure 2. 2. 3D gear pair generated in KissSoft

A simple are profile flank modification (crowning) was selected (Bergseth & Björklund, 2010) and crowning modification took place in the KissSoft platform. A definition of the crowning parameters is given in Figure 2.3.

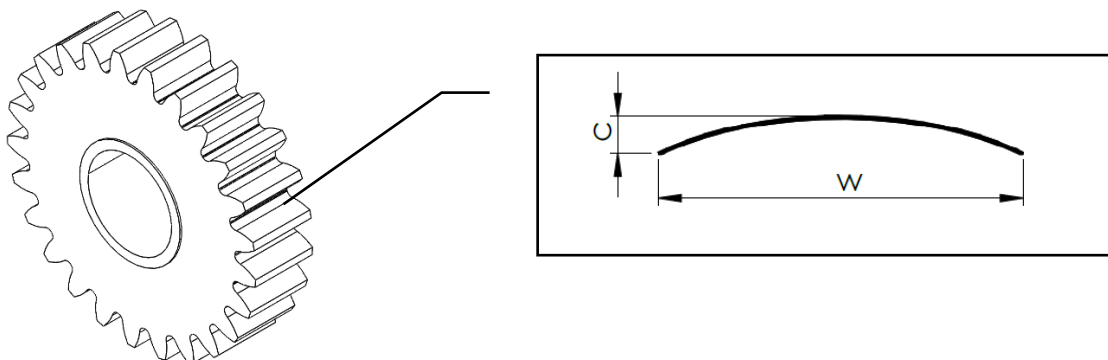


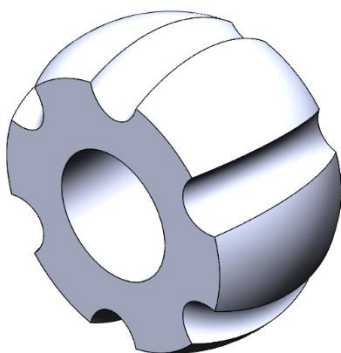
Figure 2. 3. Crowning parameters. C – crowning amount, w – tooth width

In this scheme, the crowning modification symmetrically removes the material starting from the sides, progressing towards the center. For this particular study non-dimensional crowning of $3.6 \mu\text{m}/\text{mm}$ (this corresponds to a typ. $20 \mu\text{m}$ crowning for a 5.5 mm module gear) was analyzed. As per standard industry practice, the crowning modification was applied to the pinion only.

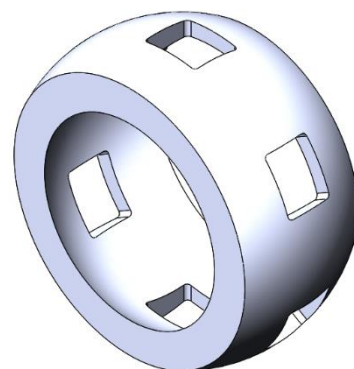
The proposed design of the misalignment-insensitive gearing transmission is based on the Rzeppa joint - or constant velocity ball joint - a concept that is widely used by automobile manufacturers (Figure 2.4). The additional details allowing the assembly of the joint are not shown here but are described in the original patent by Rzeppa (1936). Constant velocity ball

joints enable transmitting torque between arbitrarily located shafts. Main features of this implementation are circular grooves arranged in a spherical pattern, in which hardened ball elements are held by a cage and are free to roll, thus producing a self-aligning action similar to self-aligning bearings, but at the same time allowing the transmission of torque loads, due to the orientation of the grooves. These features create the desired coupling between an outer ring, which is the gear element, and an inner ring, which is fixed to the shaft.

In the presented embodiment, specifically, the number of balls and grooves is equal (in this case six) and has the same radius. Openings are created along the periphery of the inner ring so that balls could be retained in them. Grooves provide free movement of the balls along the circular periphery (in the direction of non-torque loads), whilst tangential (in the direction of torque loads) and radial movements are constrained. Like in constant velocity ball joints, sliding and rolling of the balls along the grooves allow gears to turn and obtain any angular position. Consequently, this kinematical interaction between grooves and balls provides the misalignment insensitivity of the novel design and allows its automatic adjustment to any kind of angular misalignment. In addition, the transmission of torque loads is maintained via the ball-groove interfaces, through the contact points between balls and grooves. This kind of misalignment-insensitive gears could be manufactured in different configurations in terms of ball-groove pair numbers. The amount of angular misalignment, the proposed design is able to operate at, depends on geometrical parameters of the gears, grooves, and balls.



a)



b)

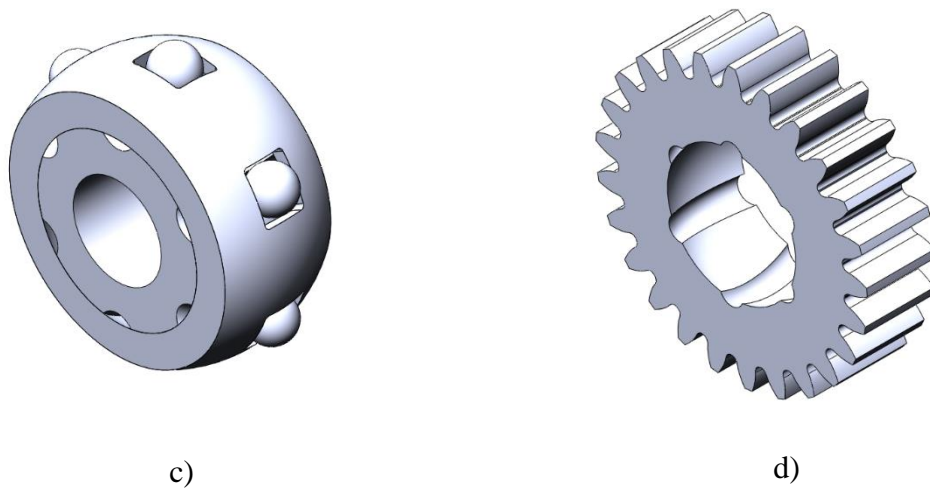


Figure 2. 4. Proposed design with Rzeppa-type joint: a) star; b) ball case; c) assembled inner part; d) gear (details allowing the assembly of the system are not shown)

Finally, the novel gear with the compliant web was originated from the original gear set which was created in the gear modeling platform (KissSoft). The main difference being material removal from gear rim region resulting in a pair of thin inclined webs with equal thicknesses. As discussed in the previous part, Li (2012) proposed a solution against misalignment issues in the form of gear with a thin inclined web and reported abnormal stress reduction compared with the regular set of gears. Li's model has a single web while the model proposed by this work has two inclined webs with their center-lines coinciding on the gear center. The more detailed topology of the proposed gear with the thin web is given in Figure 2.5. As mentioned above two compliant web gears with different web thicknesses will participate in the study.

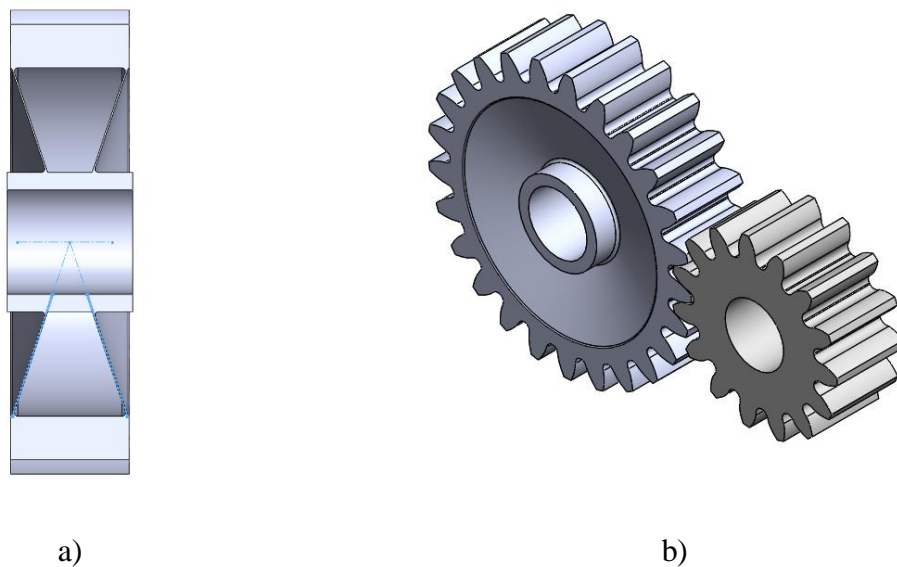


Figure 2. 5 Thin rimmed gear with the inclined web: a) section view; b) isometric view

This paper considers an in-plane angular misalignment scenario, which is known to normally produce problems. To simulate the misalignment scenario, a parametric study was created in the SolidWorks 3D modeling platform, so that any kind of yaw misalignment scenario could be achieved (Figure 2.6).

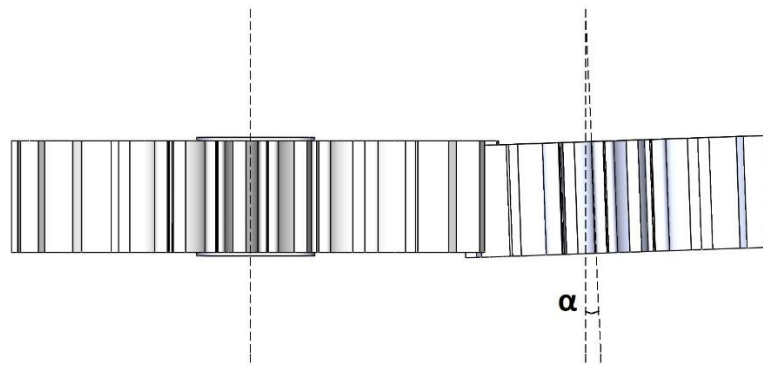


Figure 2. 6 Geometric models of misaligned gears (α is the misalignment angle)

Simulations were performed for different misalignment values for the benchmark, flank modified and proposed designs (models A-E), for misalignment values of 0° (no misalignment), 0.1° and up to 0.2° (in-plane).

2.3 Numerical modeling

In this study, FEA simulations found its implementation, which has been confirmed by several authors to produce valid results, as discussed in the introduction. Quasi-static models were used to estimate load distribution, TE, and maximum stress values and identifying load concentration areas in the benchmark, crowned and proposed models. The simulations took place in ANSYS Mechanical.

To improve the solution efficiency, the system model geometry of gears with a kinematical joint was simplified, considering the only interfaces between the gear teeth and the balls and outer grooves, where the maximum stresses are expected. The assembled inner part was replaced by a simplified model having the same external envelope, but no moving parts, as seen in Figure 2.7. This simplification is consistent with the kinematics of the Rzeppa joint and does not harm the generality of the obtained results for the studied gear.

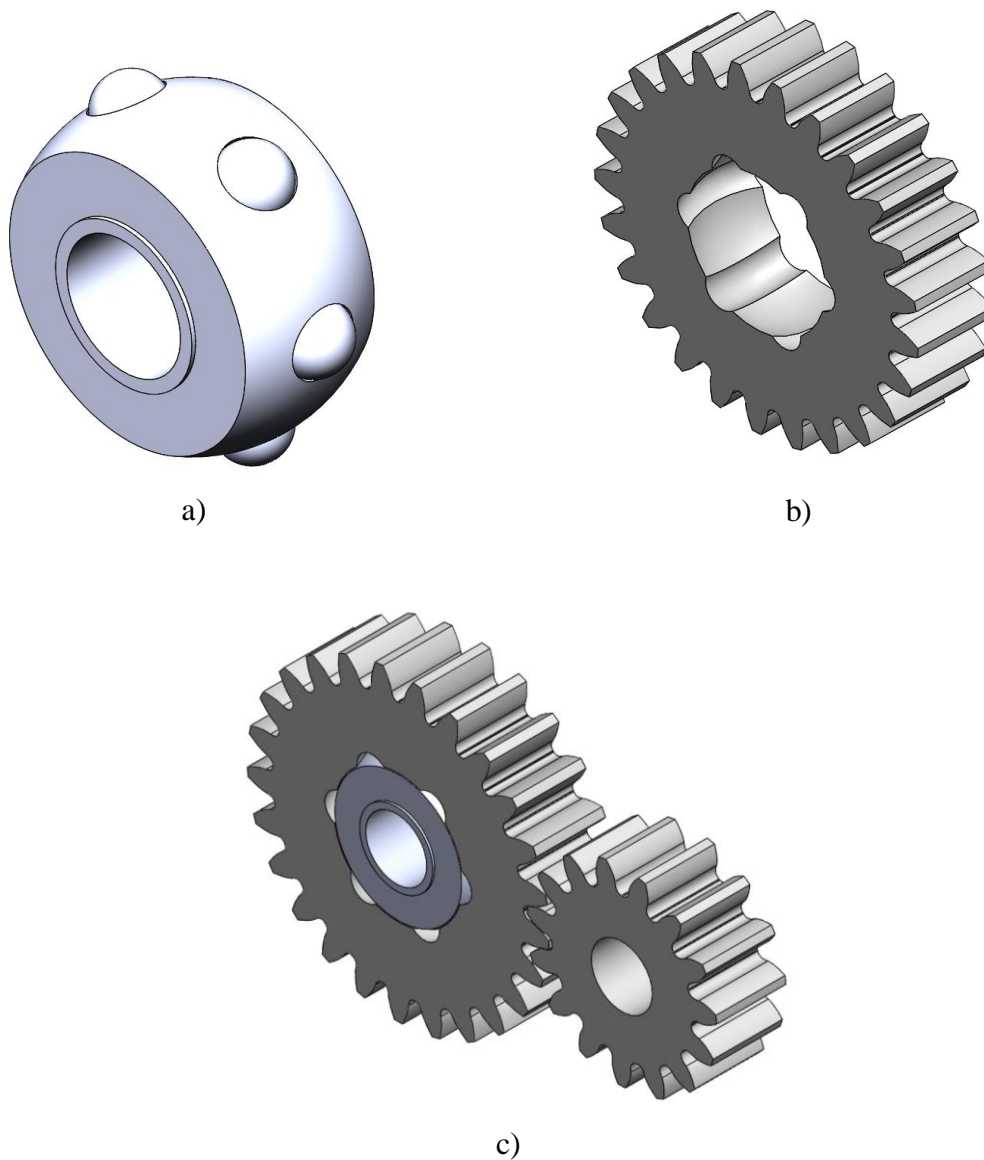


Figure 2. 7 Main components of the simplified design used in this study: a) inner ring with spherical balls fixed along its periphery; b) gear with circular grooves; c) isometric view of the overall system with the pinion

Boundary conditions

The benchmark model (Model A), a model with crowning (Model B) and a web modified model (Model D, E) were assigned the same boundary conditions, consistent with the actual operation of the gears. In both cases, the gear rotates around the cylindrical support under an external torque, which corresponds to 20% of the critical load (calculated on KissSoft), meanwhile, the pinion was fixed to oppose the rotary movement of the gear. Relatively low torque magnitude compared to the allowable margin was chosen by considering a further increase in loads in misaligned scenarios. The contact area between gear and pinion was given frictionless behavior (Figure 2.8).

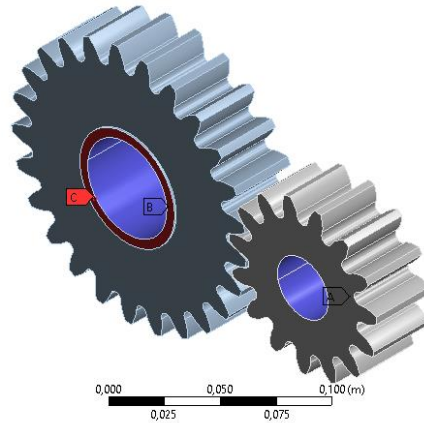


Figure 2. 8 Boundary conditions of the benchmark and crowned system (Models A, B, D, and E)

For the proposed design (Model C), boundary conditions are more complicated compared with the benchmark model due to the presence of different contacts to be properly defined. First, the contact between balls and the outer ring grooves is defined as frictionless, to compensate for the inability of the balls to rotate in the simplified model. Also, the pinion and gear are connected by a frictionless interface. As with models A and B, the pinion is fixed, while the inner ring was free to rotate around its cylindrical support under an external 100 Nm torque (Figure 2.9).

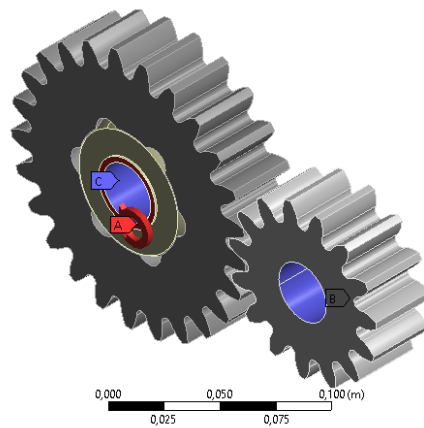


Figure 2. 9 Boundary conditions of the proposed design (Model C)

2.4 Meshing

The accuracy of FEA results, particularly in the case of contact problems, is highly dependent on the quality and size of the FE mesh. Thus, to find the appropriate parameters for the FE mesh, a sensitivity analysis was conducted using a multi-zone approach. The reference point to measure tooth stress is located 4 mm away from the tooth edge along the contact line

with coordinates (64.2mm, 1.1mm, 13mm, point X). Meanwhile, for the ball-groove interference, the reference point coordinates are $x=36.7\text{mm}$, $y=4.3\text{mm}$, $z=0\text{mm}$ (point Y), and point Z with coordinates of (68mm, 8.5mm, 10mm) which corresponds to the flank modified design. Moreover, for the compliant web design, the reference point T was selected for mesh sensitivity analysis (64.2mm, 1.1mm, 13mm) (Figure 2.10). The nominal element size on the primary contact interfaces was progressively reduced in subsequent iterations until the acceptable error in the reference points is obtained and convergence occurred. Element size is given in the form of a fraction of the normal module (Figures 2.11-2.14).

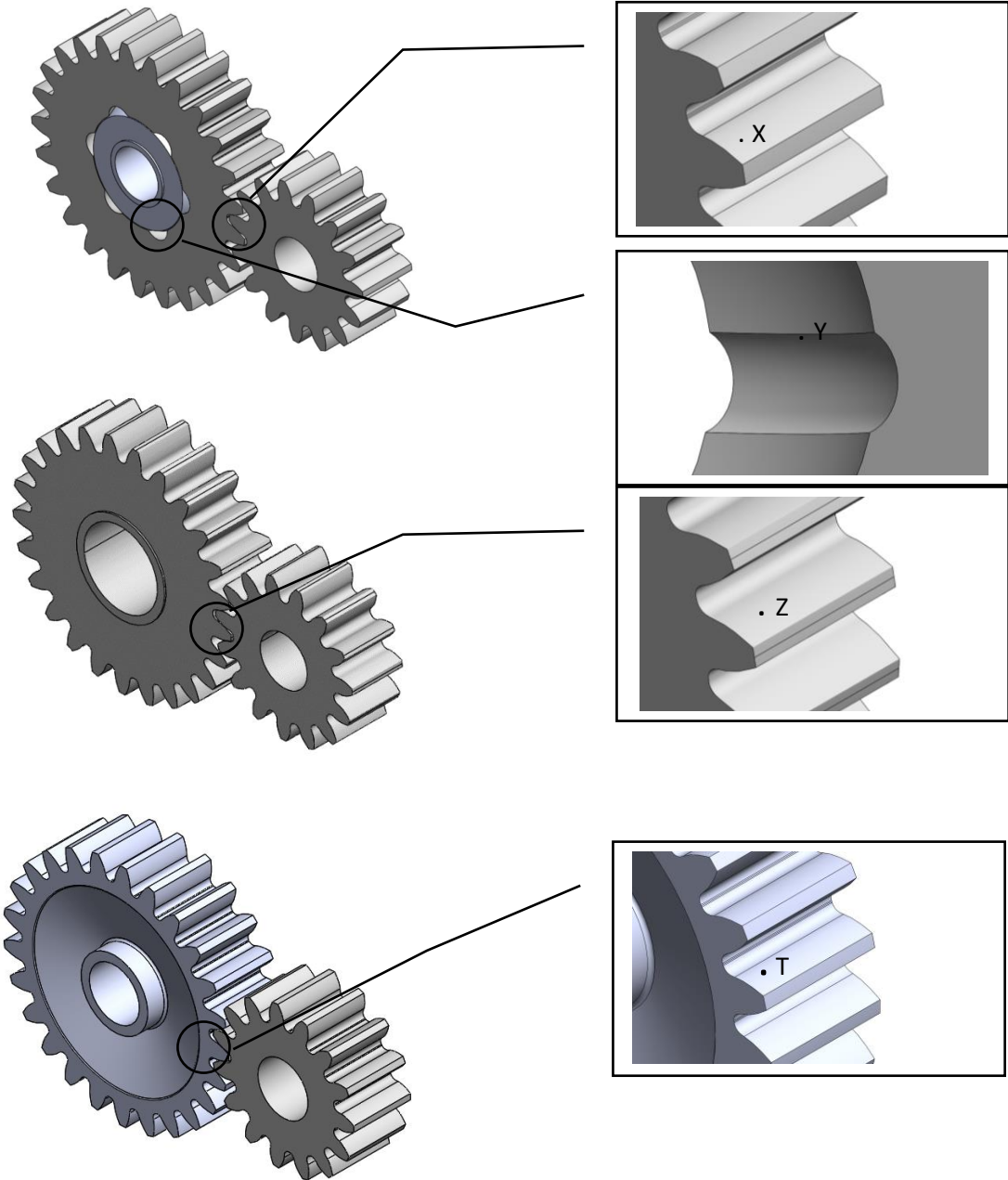


Figure 2. 10 Location of the reference points (points X, Y, Z, T)

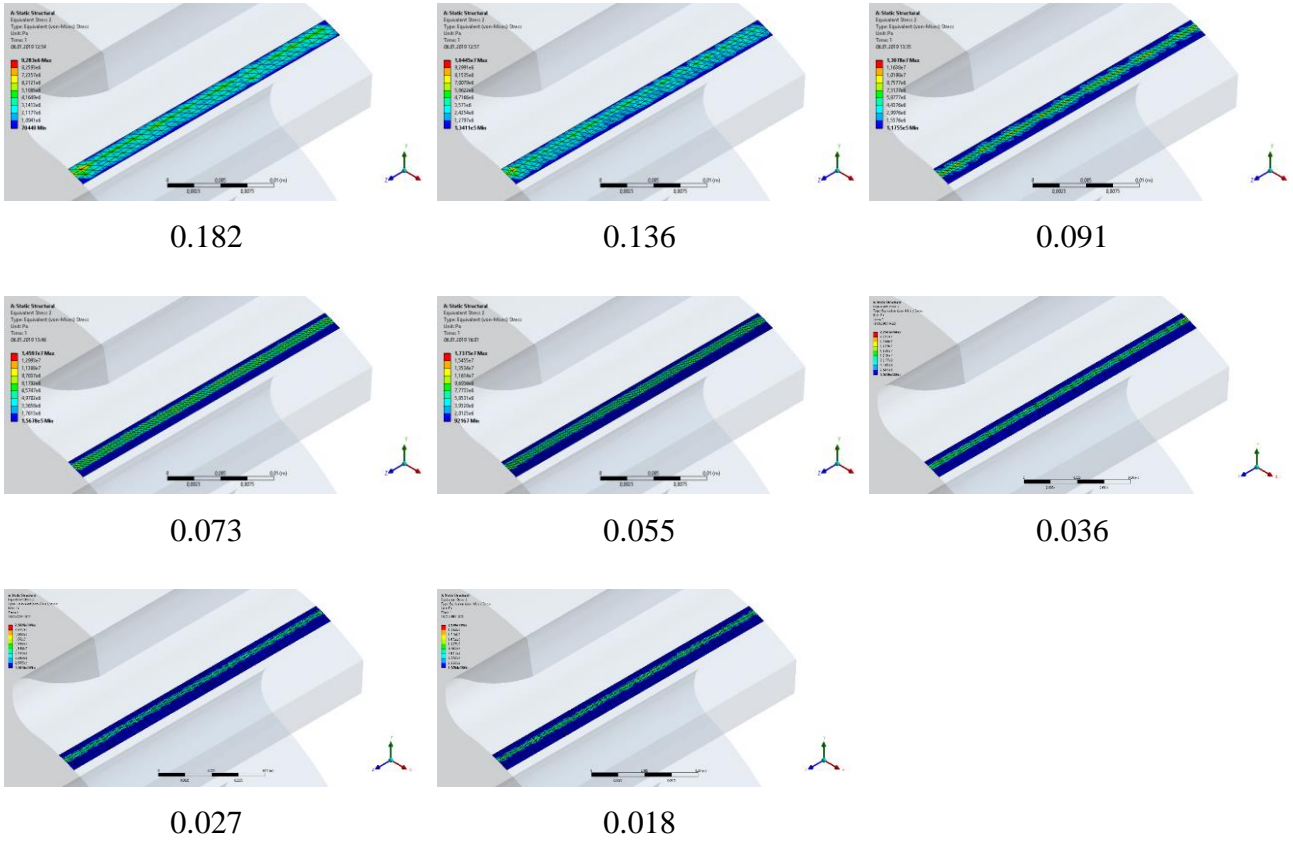
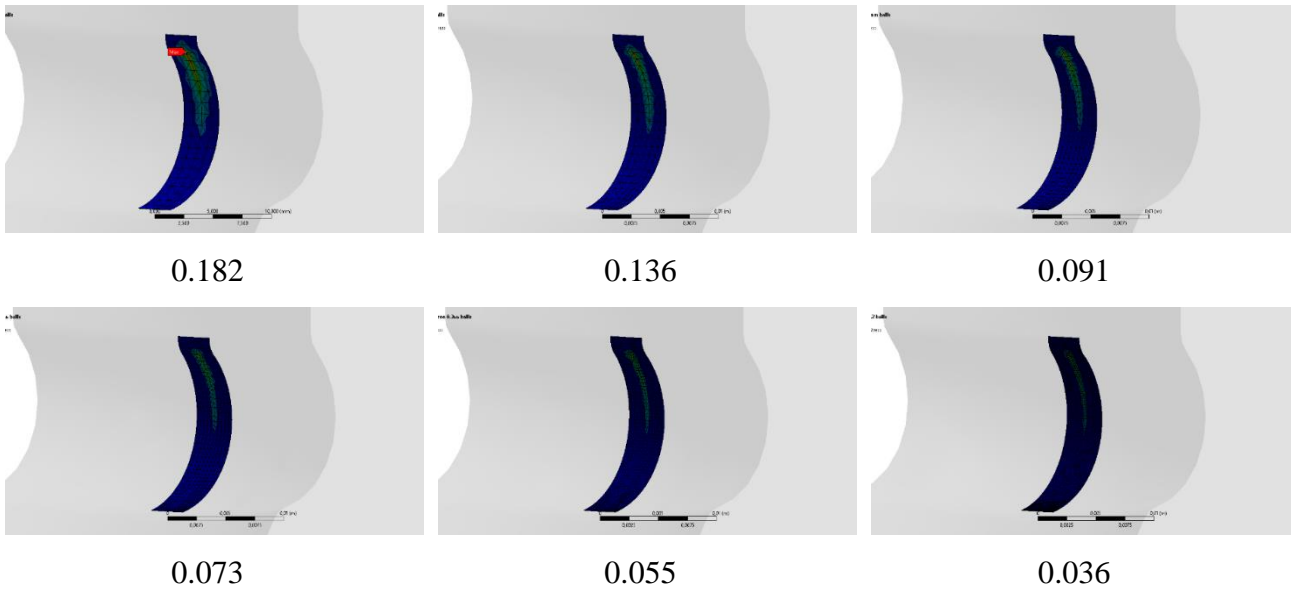
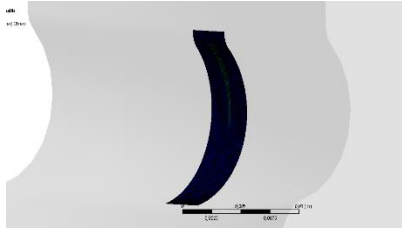


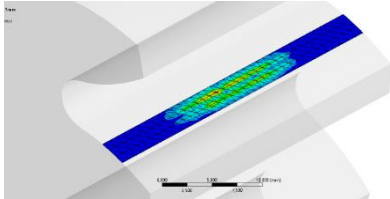
Figure 2. 11 Meshing along the tooth mesh contact (Point X, as a fraction of the normal module)



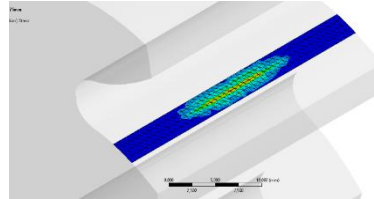


0.027

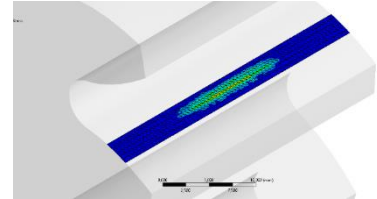
Figure 2. 12 Meshing of groove-ball interference (Point Y, as a fraction of the normal module)



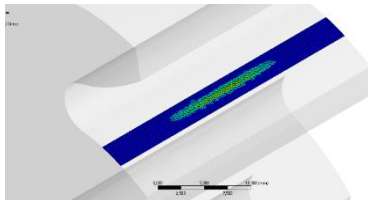
0.182



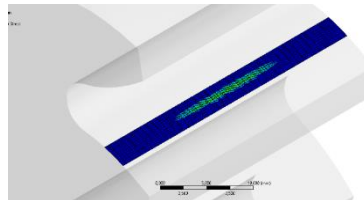
0.136



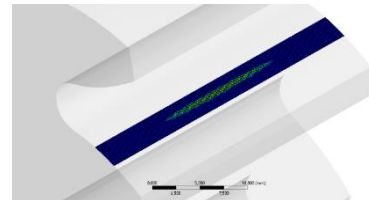
0.091



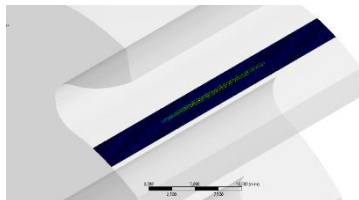
0.073



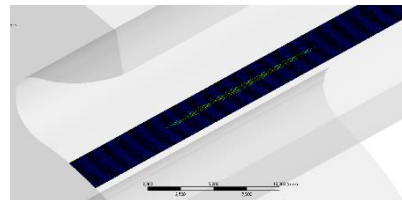
0.055



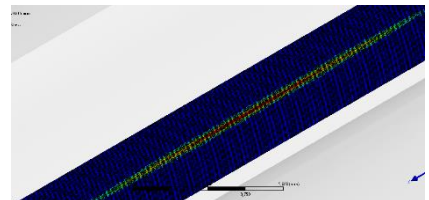
0.036



0.027

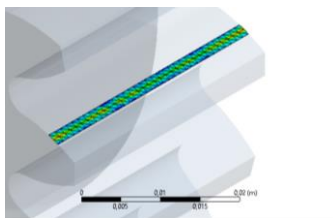


0.018

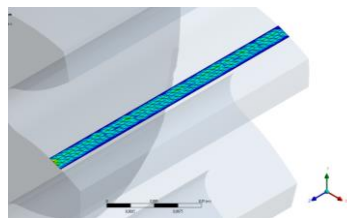


0.009

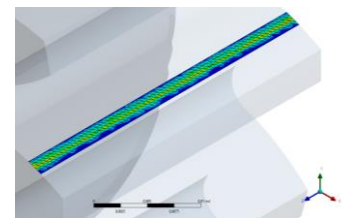
Figure 2. 13 Meshing of tooth mesh contact line (Point Z, as a fraction of the normal module)



0.182



0.136



0.091

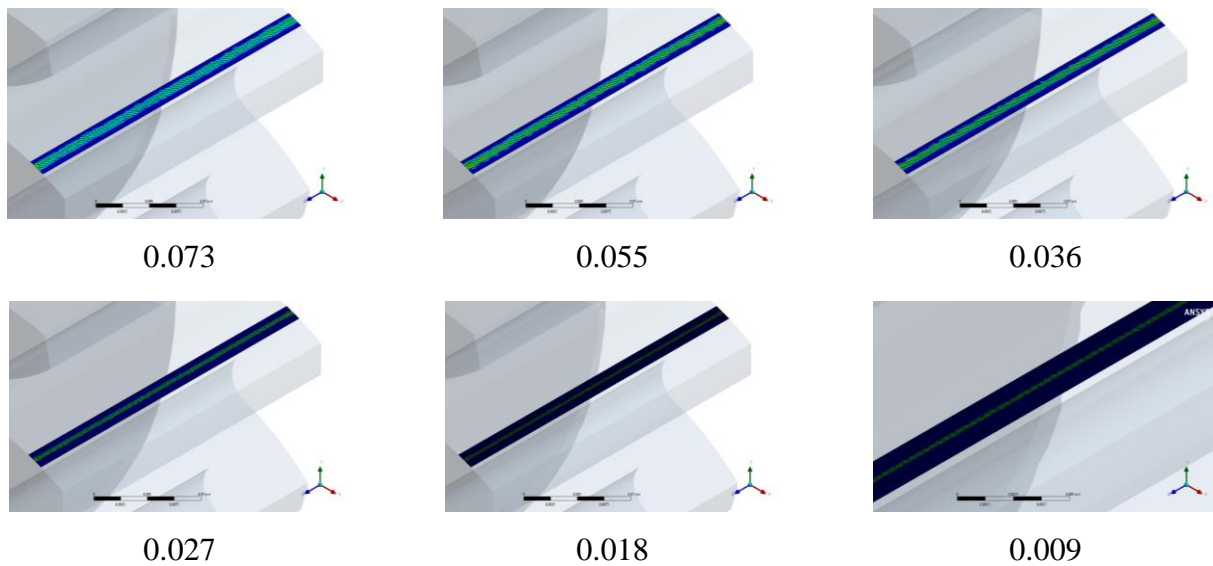


Figure 2. 14 Meshing of tooth mesh contact line (Point T, as a fraction of the normal module)

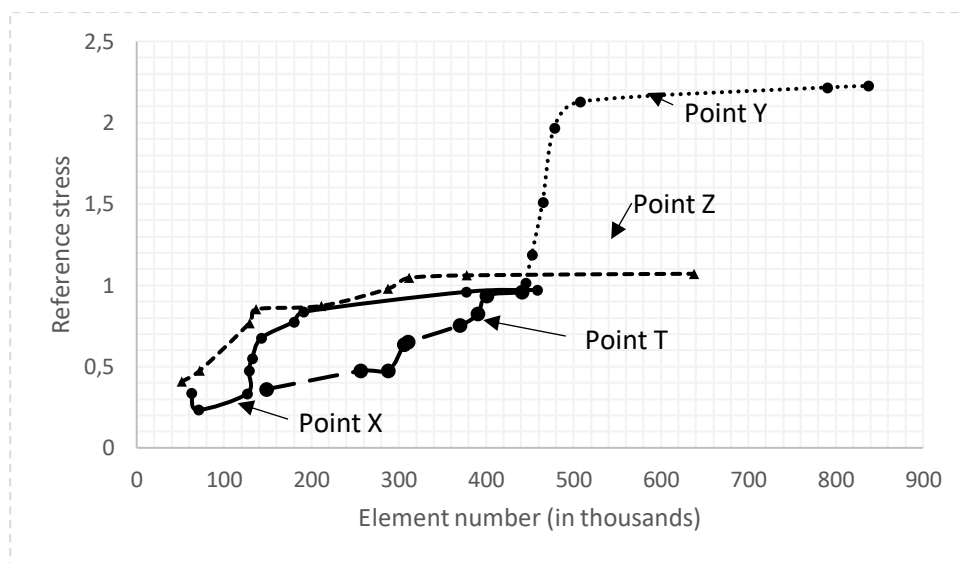
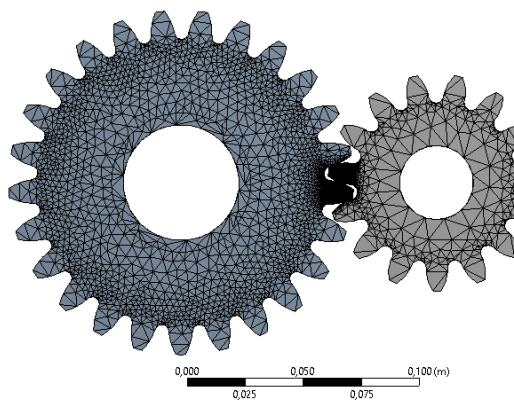
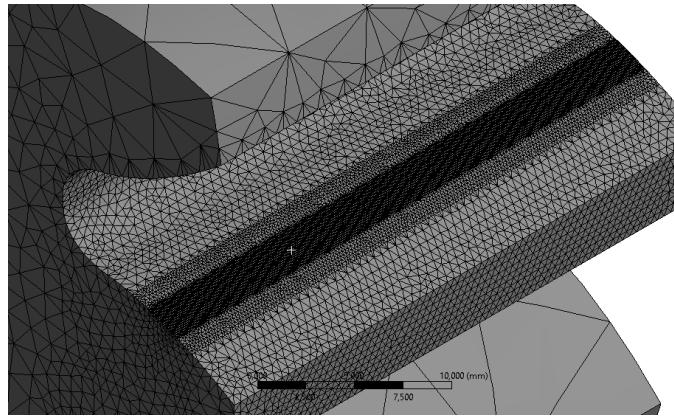


Figure 2. 15 Mesh sensitivity analysis

From the mesh sensitivity analysis graph from Figure 2.15, for points X, Y, Z, and T it is apparent that as mesh density/element number increases the reference stress values begin approaching its asymptotical margin, meaning the reference stress values appear to converge with reducing errors in subsequent iterations. The model with crowning modification required more refined meshing in contact areas comparing with other designs, because of the complex flank modification that needs to be accurately defined. Final meshed models are given in Figures 2.16-2.19.

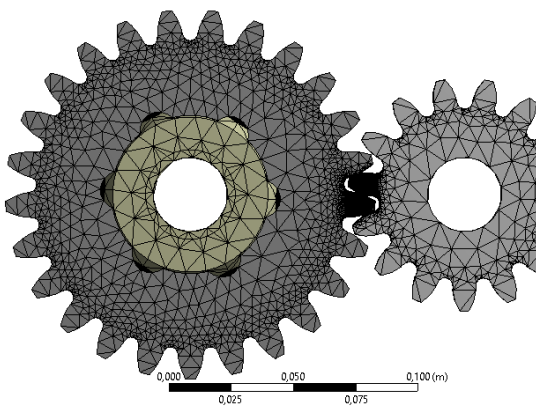


a)

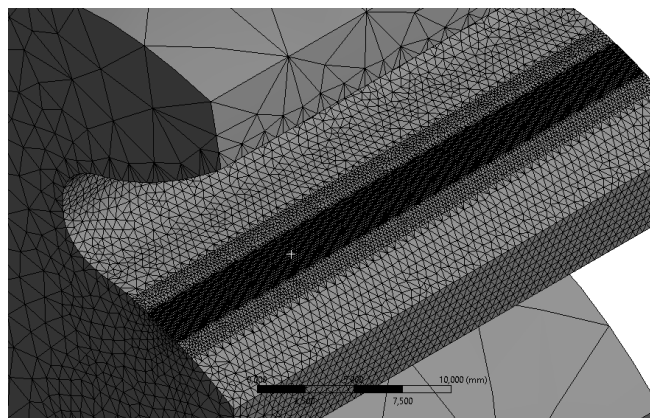


b)

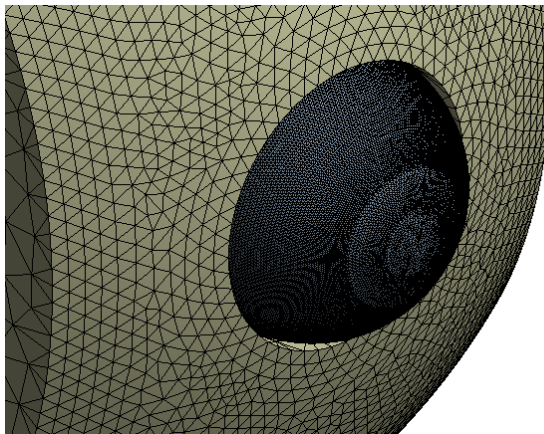
Figure 2. 16 Mesh elements of the benchmark design. a) side view; b) tooth flank,



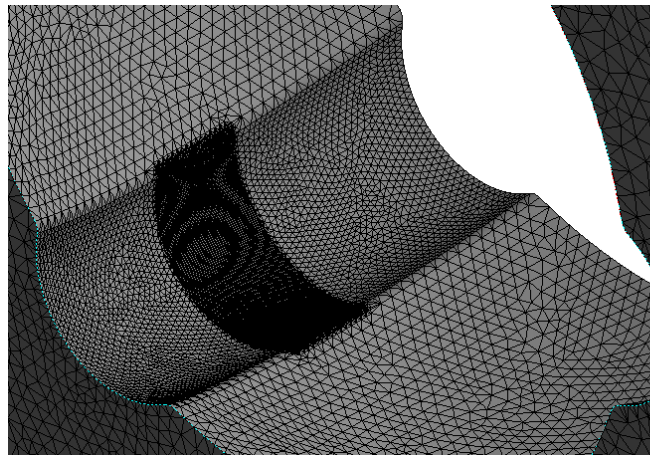
a)



b)



c)



d)

Figure 2. 17 Mesh elements of the proposed design a) side view; b) tooth flank; c) ball; d) groove.

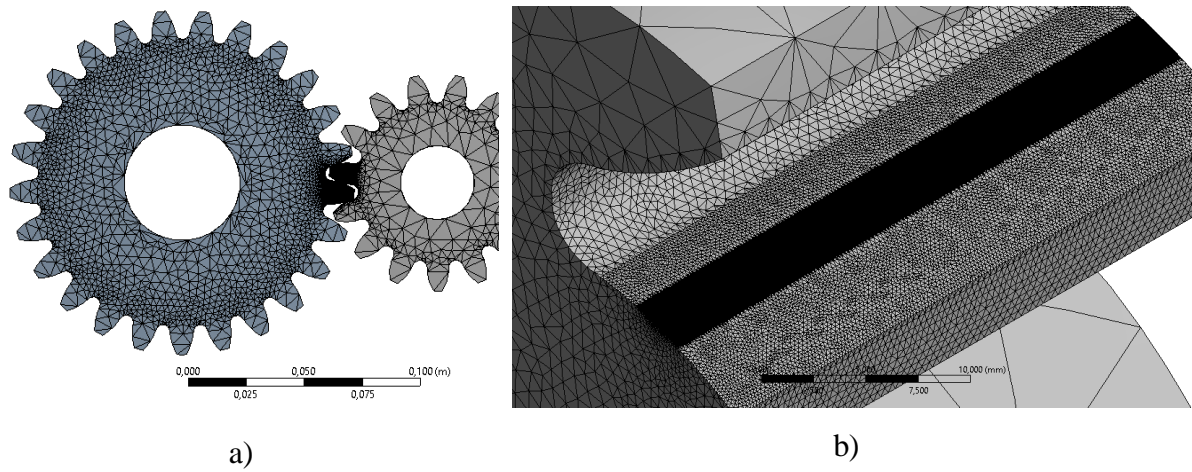


Figure 2. 18 Mesh elements of the crowned design. a) side view; b) tooth flank.

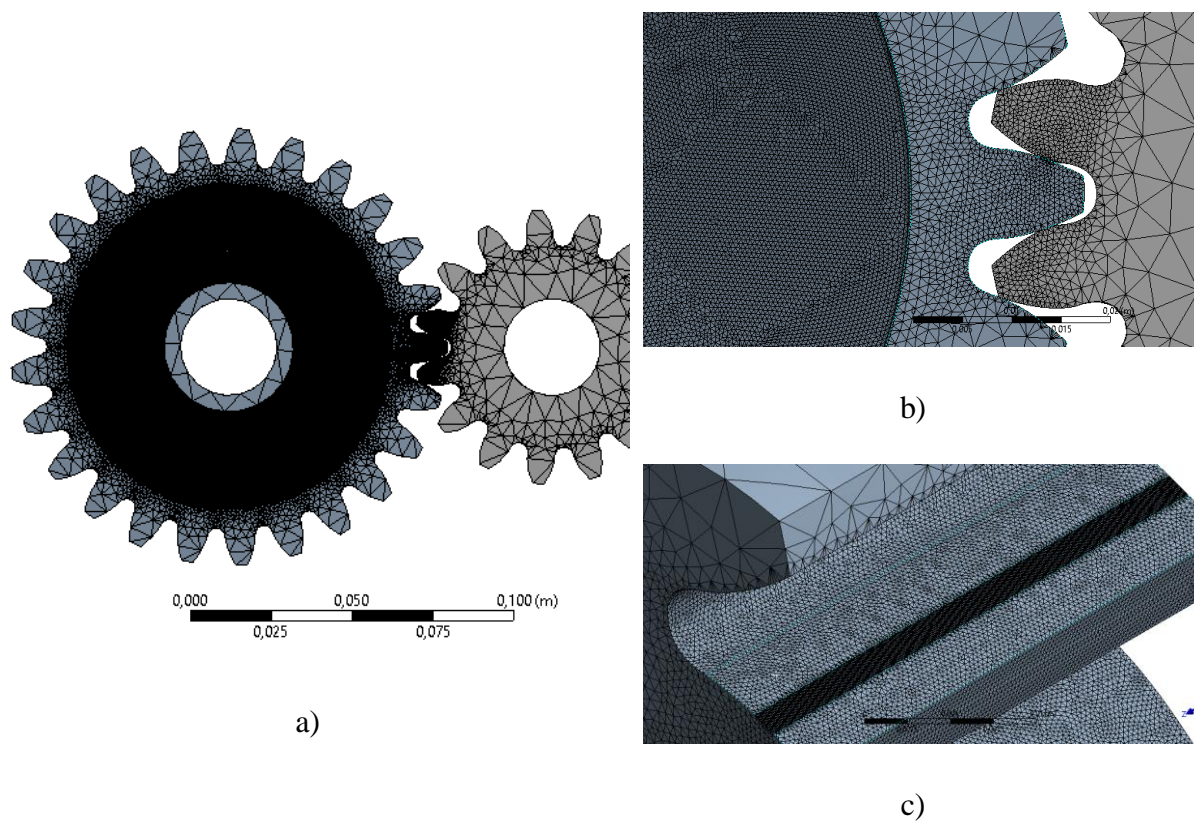


Figure 2. 19 Mesh elements of the web modified design. a) side view; b) web and meshing area; c) tooth flank.

2.5 Transmission error (TE) calculation

TE is the deviation between the idealistic (reference) and the actual position of gear, using its mating gear as a reference, and is calculated in the following way:

$$TE = \theta_1 - \theta_{1,ref} \quad (1)$$

$$\theta_{1,ref} = \frac{z_2}{z_1} \theta_2 \quad (2)$$

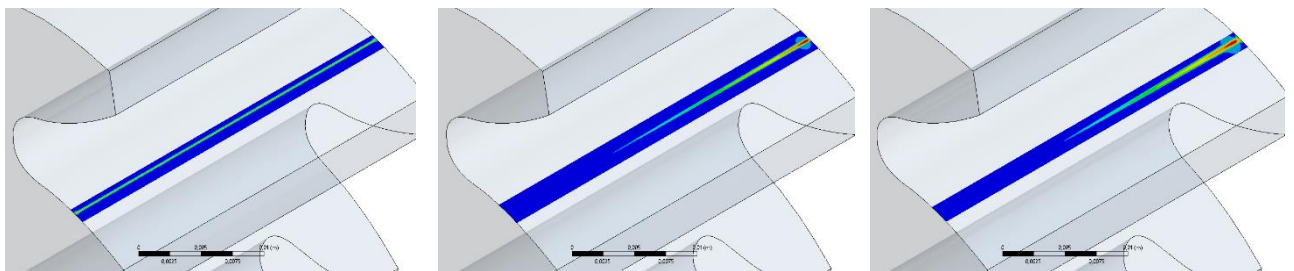
Where TE stands for transmission error, θ_1 and θ_2 represent the angular position of each gear in a pair, respectively, and z_1 and z_2 are corresponding numbers of teeth.

Mostly, the transmission error is a result of a bending of a gear tooth under a load and contact characteristics. Therefore, sufficiently accurate meshing is required to capture the combined effects of Hertzian stiffness and the bending and foundation stiffness of the gear teeth, as well as the load distribution due to the simultaneous engagement of multiple teeth for part of the mesh cycle. At the same time, due to the integral nature of the displacements that accumulate to produce the TE, the results are much less sensitive compared to those for stress assessment.

2.6. Results and discussion

2.6.1. Benchmark model (Model A)

The benchmark system with different angular misalignment went under simulation first. As expected, in the case of zero misalignment, the stress distribution along the contact line was continuous and even. However, as gears get misaligned relative to one another, as predicted, the maximum stress value along the contact line increased rapidly, mainly concentrating on the tooth edge (Figure 2.20).



$\alpha=0^\circ$

$\alpha=0.1^\circ$

$\alpha=0.2^\circ$

Figure 2. 20 Contact stresses for benchmark design (Model A) for different misalignment values

2.6.2. Crowned gears (Model B)

Since flank modification is an existing remedy to gear misalignment, gear pair with a pinion crowned tooth profile was considered in the study (Figures 2.21). Both gears experienced less stress in comparison to conventional gear. However, due to a rapid decrease in the contact area, the maximum stress increased as well, but it did not exceed load values obtained in the case of the misaligned benchmark system. It should be noted that the implementation of crowning eliminated corners that can be subjected to high stresses. Therefore, the stress profile obtained an ellipse shape with a central area mainly exposed to the loads. Moreover, this ellipse-shaped area tends to shift sideways as the misalignment angle increases and at 0.2° misalignment almost reaching the edge of the tooth. Thus, a further increase of misalignment angle leads to the development of edge contact similar to non-crowned gears, making them vulnerable to misalignment.

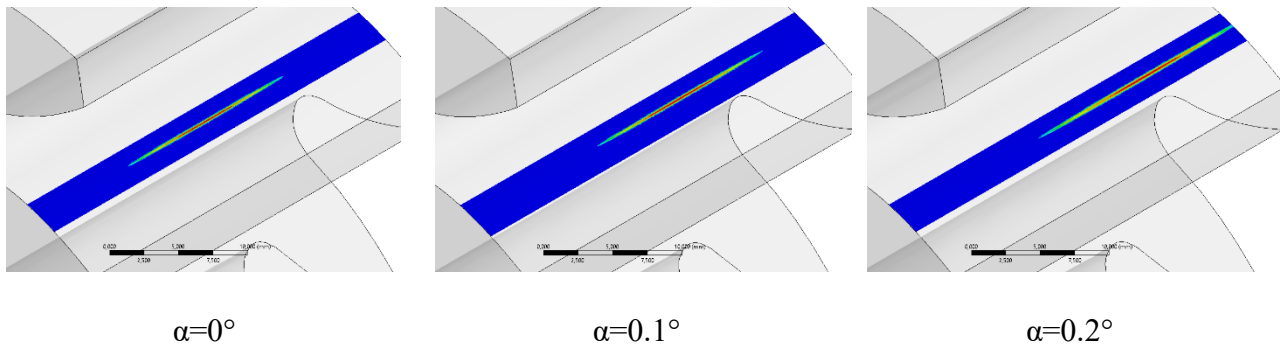


Figure 2. 21 Contact stresses of crowned design (Model B, crowned) for different misalignment values

2.6.3. Proposed design (Model C)

Numerical simulations on the novel gears with integrated Rzeppa joint revealed the ability of the proposed design to adapt to the angular displacement of the pinion and adjust itself automatically to any misaligned position (Figure 2.22). Simulation results demonstrated a smooth allocation of loads along the contact line. It proves the hypothesis that the proposed design with the kinematical joint can solve misalignment issues of spur gear pairs in the same way as self-aligning bearing mitigates improper shaft alignment (Figure 2.23). Simulation results clearly show the center of rotation and entire gear turns around the centerline. Moreover, in the case of the proposed model, the maximum stress shifted to the ball-groove interface.

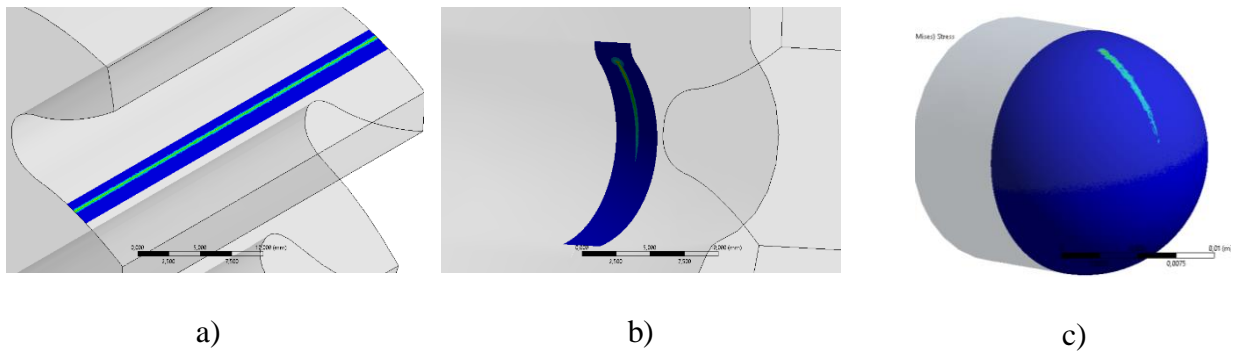


Figure 2.22 Proposed design (Model C) at any misalignment (results were identical). a) Tooth contact stresses; b) Contact stresses inside groove; c) Contact stresses on the ball.

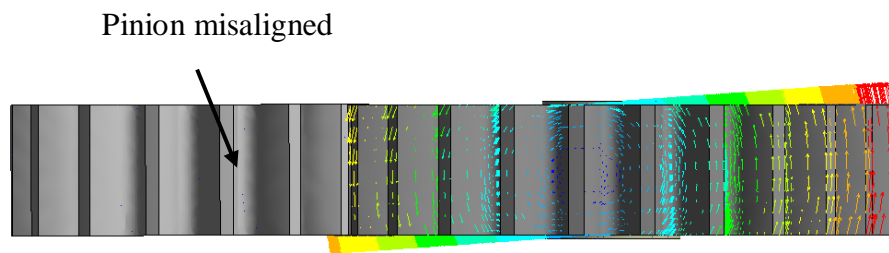
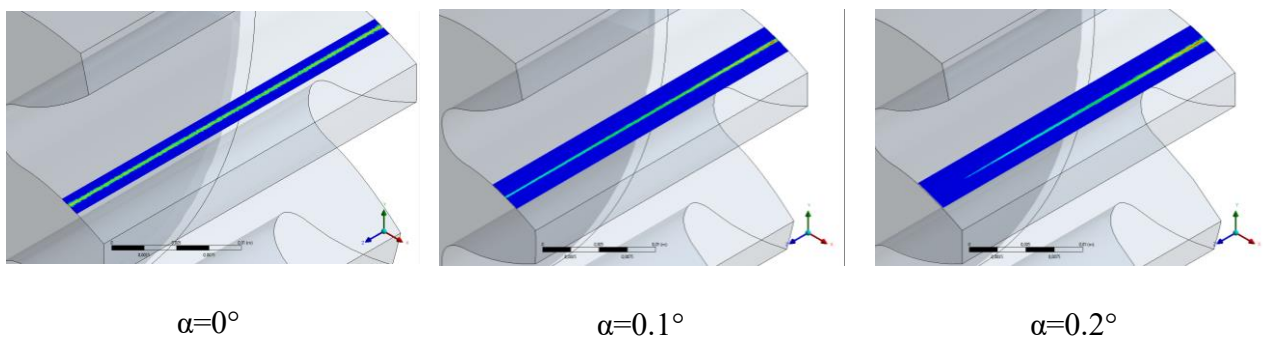


Figure 2.23 Vector displacement field, showing the automatic realignment action of the proposed design (Model C-gear adjusts its orientation to the fixed pinion)

2.6.4. Gear with compliant web (Model D and Model E)

According to simulation results by means of FEA, the proposed design with thin compliant web shows the capability to mitigate gear misalignment to some extent. In case of misalignment, the stress pattern is noticeable longer for the flexible web model than for the benchmark model at identical misalignment angles. Not surprisingly, due to better flexibility of thinner web the 0.2mm model shows better performance comparing to 0.4mm analog, which can be observed from stress patterns. In addition, for both cases, despite shifted stress footprint, no extremely high-stress concentration areas were observed (Figures 2.24-2.25). However, the flexible web designs are unable to alleviate misalignment issues as successfully as the design with the Rzeppa joint.



$\alpha=0^\circ$

$\alpha=0.1^\circ$

$\alpha=0.2^\circ$

Figure 2. 24 Gear with compliant web with 0.2mm thickness (Model D)

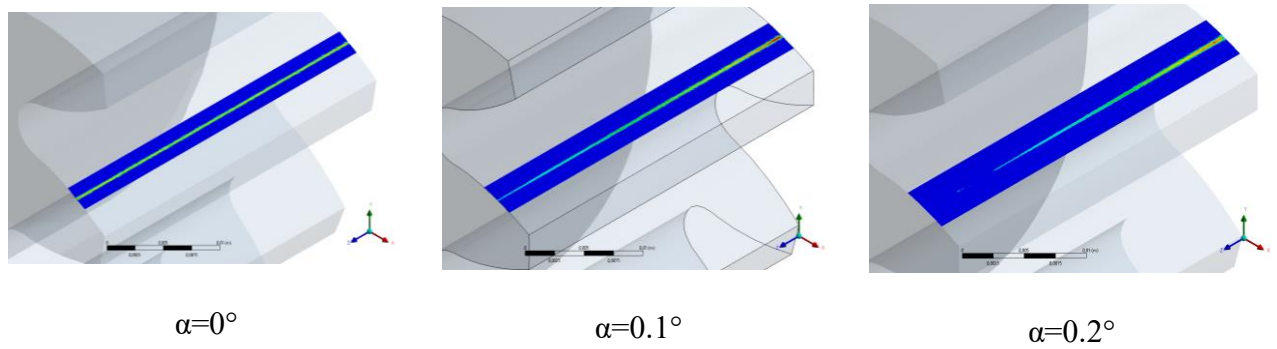


Figure 2. 25 Gear with compliant web with 0.4mm thickness (Model E)

In addition, deformation results for the compliant web design are consistent with the stress results. The vector displacement field for the flexible rim design indicates misalignment adjusting capability as the Model C with a kinematical joint, where the instantaneous center of rotation could be detected (Figure 2.26).

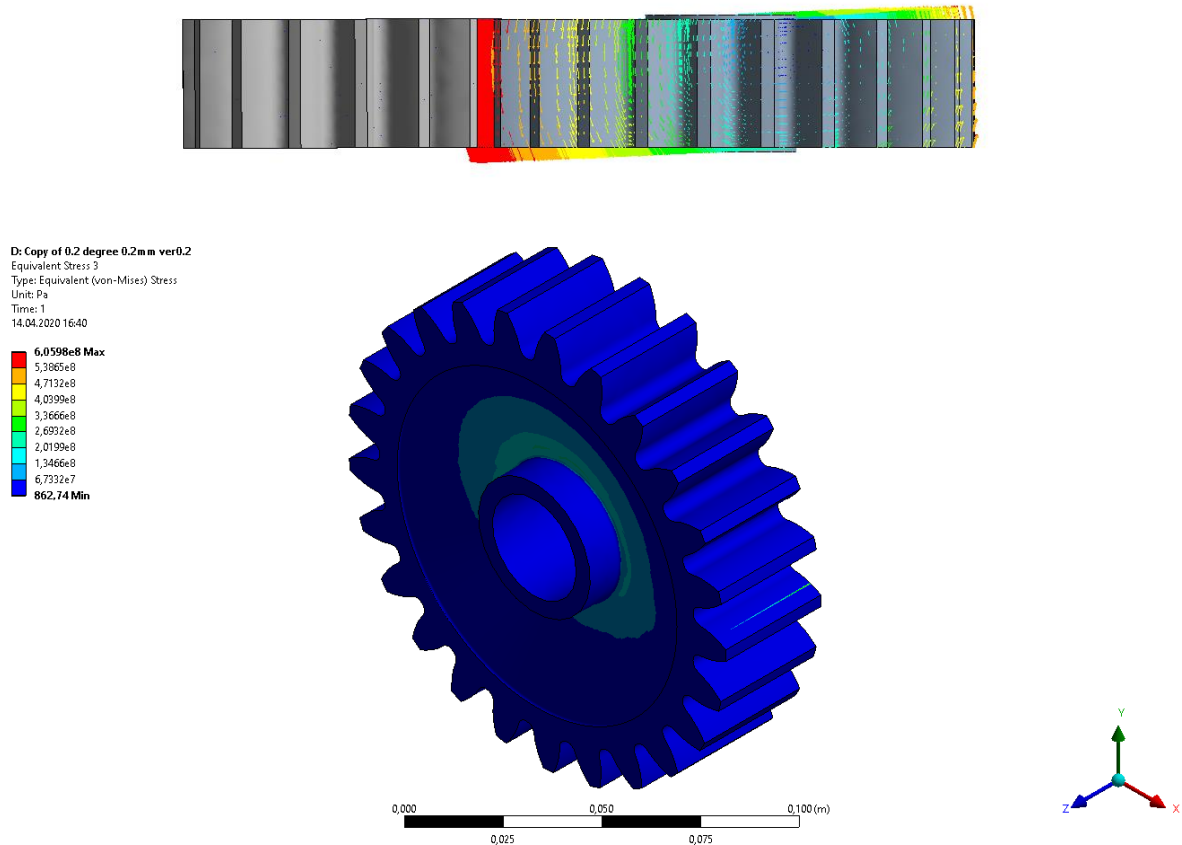


Figure 2. 26 Deflection of the thin compliant rim

First of all, as confirmed by quasi-static FEA simulations, the proposed model with constant velocity ball (Model C) joint displays the most superior capability to adjust to any kind

of misalignment, by obtaining a properly aligned position between mating pinion and gear. The load sharing pattern along the primary contact line remains continuous and uniform for all range of misalignment angles similar to an accurate alignment case. In contrast, in case of misaligned regular gears or Model A load pattern becomes non-uniform with extreme stress concentration points emerging on the tooth edge, meaning the vulnerability of the spot to micro-pitting, wear and chipping, which successively lead to premature breakdown. In the case of existing gear misalignment solution, the model with flank modification or crowning (Model B) demonstrated moderate performance against the misalignment issue, mainly due to exclusion of acute gear tooth corners where highly concentrated stresses tend to emerge. Therefore, crowning only allows translation of the stress concentration region towards the tooth center. However, there is still a possibility of obtaining harmful edge stresses, particularly at larger misalignment angles; thus meaning in case of gear crowning, there is an unavoidable trade-off between possible stress reduction and misalignment insensitivity. For design models with thin web topology (Models D and E), FEA results demonstrated a decent level of effectiveness against gear misalignment. Despite obtaining a similar load sharing pattern along the primary tooth contact line compliant web gears deal with the alignment error in a much better manner compared with the benchmark (Model A). Unlike to misaligned regular spur gears, the flexible thin web enables more delicate stress sharing for a larger area, with thinner analog showing more superior results.

Figure 2.27, demonstrates the stress comparison between the models considered in the study. Stress magnitudes are given in a form of nominal non-dimensionalized stress value as a ratio to the tooth stress of non-misaligned regular gears (Model A). For the misalignment insensitive gear with Rzeppa joint topology, two stress results were reported: the primary contact area between teeth and the ball-groove interface borrowed from the original kinematical joint. The Ball-groove interface is assumed to experience increased load values due to geometrical features. First, in the case of regular gears (Model A) stress magnitude increases drastically as gears become misaligned, showing a strong correlation between misalignment magnitude and the load experienced by the teeth. Crowned gears (Model B) can mitigate the negative effects of misalignment somewhat as revealed by numerical simulations. However, since altering tooth surface lead to contact area reduction, despite retaining steadiness, there is a noticeable increase in stress graph. It should be noted since misalignment magnitude becomes more severe, there is a change of edge stress development, which causes rapid stress increase. Unlike the previously mentioned design of regular spur gears and with thin web topology, the proposed model undergoes constant tooth stress for the given range of misalignment angles

(Model C, the tooth). Apart from uniform tooth stresses, the proposed model develops highly concentrated stress location on the ball-groove interface, which approximately two times than of tooth contact stress (Model C, ball-groove). Nevertheless, according to the stress graph, this value remains constant throughout the given range and does not show any signs of fluctuations; furthermore, the risk of fatigue issues could be mitigated by appropriate material selection such as bearing ceramics. Replacing the ball-groove interface material might be a suitable option, due to the absence of large sliding motion between parts, and only small reciprocal movements exist in the interface. For the case of compliant web gear (Model D and E), like the benchmark system (Model A), they resemble its behavior and show linear dependence between misalignment angle and stress results, but it's clear that they experience fewer stress loads, with smaller gradient.

Comparing all design types, it could be noted that based on the stress results as misalignment angle increases, the magnitude benchmark stress surpasses ball-groove stress at an angle approximately 0.09° and continues to raise. Whilst, compliant web gear with 0.4mm thickness exceeds this value at 0.12° , and in 0.2mm model stress magnitudes become larger than the ball-groove value at 0.19° , making the proposed model with Rzeppa joint the most effective in further misalignments. In addition, apart from misalignment, bucking could become an important issue for flexible web designs, because of thin web walls. Anyway, the main purpose of the misalignment insensitive gearing was to reduce adverse effects of alignment error in gears and decrease abnormal tooth stress values by making stress patterns more uniform and continuous which could be achieved by the application of kinematical joint.

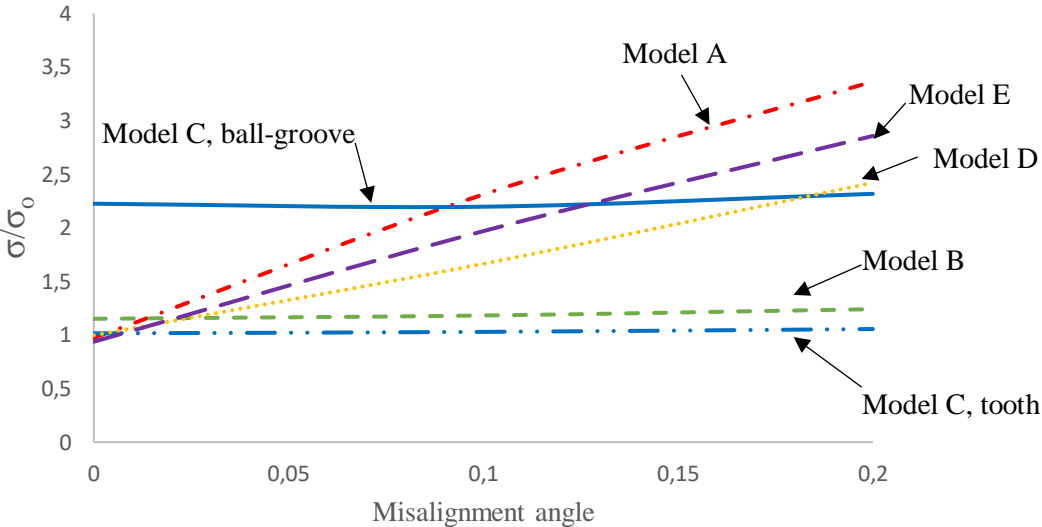


Figure 2. 27 Non-dimensional stress plot along the contact line for various designs.

(Here: Two stress curves are reported for the proposed design (model C): Blue line with double dots represents the stress at the tooth contact and is comparable to the lines for the benchmark (model A, dashed line with dots) and crowned gears (model B, green line); The solid blue line represents the maximum stress at the ball-groove contact. Stress results for models with a compliant web are presented yellow line (Model D) and dashed violet line (Model E), respectively)

Static TE was calculated for the regular gears (benchmark design) and proposed design with the kinematical joint for a single mesh cycle (Figure 2.28). There is a clear dissemblance between investigated TEs of the investigated model. For the zero-misalignment scenario, regular gears, as mesh stiffness varies, the TE graph fluctuates between specific upper and lower boundaries. Furthermore, misalignment angle growth causes TE amplitude to increase significantly, meaning that regular spur gears are negatively impacted by misalignment. This increased TE becomes a reason for increased noise generation, excessive vibrations, and other undesirable consequences. On the other hand, the average TE magnitude of the model with the mechanical joint was 9 times higher, however, no significant oscillations were observed on the graph. This increase is probably caused by ball-groove interfaces, which in fact, play the role of an additional group of spring connections. In the case of regular gears, at maximum misalignment angle, TE amplitude increased by 5 times, whereas for the proposed design it stayed constant, independently from misalignment angle. Therefore, their correlation indicates almost the total insensitivity of the kinematical joint design to misalignment, unlike conventional gears.

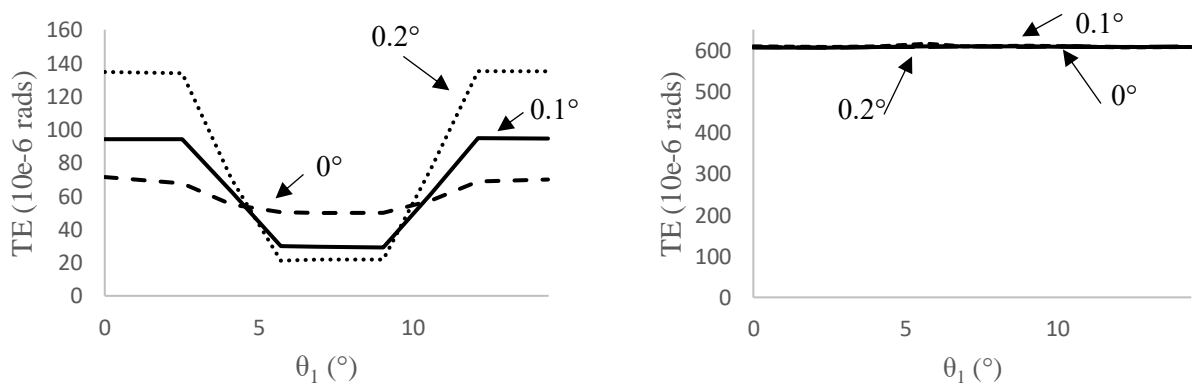


Figure 2. 28 Static TE for the benchmark (left) and proposed (right) designs over one mesh cycle, as a function of the gear position θ_1 .

The computational results prove the proposed model of the gearing transmission with the universal joint can eliminate detrimental effects of gear misalignment by automatic

adjustment of the angular position of a misaligned gear. The proposed design is also shown to achieve lower stresses even compared to flank-modified (crowned) and compliant web design solutions. While contact stresses at the gear tooth interface remain unaffected, the trade-off is a somewhat increased stress at the contact surfaces between the balls and the groove of the Rzeppa joint.

Chapter 3 – Bearingless floating-carrier compound planetary gearbox

3.1 Literature review

Del Castillo (2002) developed an analytical method to calculate the efficiency of planetary gear systems. The structure of the gearbox system may vary as well as the type of gears itself. Gear types may take the following forms: spur, helical, herringbone, bevel, gear hob, worm, and hypoid. Each type of gear has its advantages and disadvantages, such as efficiency, cost, noise, complexity.

Several research articles analyzed the reliability of the planetary gearbox. One of the common factors affecting the overall reliability of planetary gears is unequal load sharing among the gear components. The disproportionate load sharing is mostly caused by manufacturing and installation errors, deformations and gear misalignment, which are almost inevitable. For example, one study reported that for a particular planetary gear model used in helicopter applications in case of uneven load sharing among planets, the reliability factor drops from 96.762% (normal case) to 87.562% (Li, Xie, & Ding, 2017). Comparing with conventional gearboxes with spur gears mounted on parallel shafts, traditional planetary gearboxes provide higher power density (Hidaka, Terauchi and Nagamura, 1976), (Kahraman and Blankenship, 1996). High power density is achieved by splitting input torque between planets and sun gear. However, this equal distribution of a load is only possible theoretically. In reality, the unevenly split load leads to premature failure of the system. Thus, even the load sharing ability of planetary gearboxes is a significant design parameter that directly affects the reliability. Considering uneven stress distribution in planetary gearboxes, Singh (2010, 2011) developed an approach to approximate loads in planets in case of the non-uniform distribution for generic planetary gearboxes with planet numbers between three and seven. As reported by Guo, Keller,

and Lacava (2014) who studied planetary gearboxes of wind turbines in terms of their reliability, planetary gearboxes of wind turbines fail frequently, rarely reaching their full lifespan. Also, the authors claim that in the case of wind turbine gearbox, the bending moment of a shaft has more influence on unequal load sharing within the system compared with other main factors such as fluctuating mesh stiffness, nonlinear tooth contact, and tolerances, and might to premature failure of gearbox. Park et al. (2016) developed a novel transmission error based model to fault diagnosis of planetary gears.

Some studies investigated the possible implementation of flexible ring gear against uneven load sharing caused by manufacturing errors (Kahraman and Blankenship, 1996). Also, Kahraman, Kharazi, and Umrani (2003) in their study investigated a planetary gear set with thin-rimmed gear components that consider them as flexible bodies. Results show that the model with flexible components experience significantly higher tooth bending stresses compared with conventional models where gears are considered as rigid. However, adding flexible components in the planetary gearbox was found to be an ineffective solution against non-uniform load sharing between planets. Kahraman and Vijayakar (2001) claimed that a novel concept with floating sun gear was more effective compared to the flexible components solution against the uneven stress issue. Nevertheless, lately, this solution also found to be sufficient by Singh (2005). Apart from uneven stresses on planets, planetary gears suffer from noise and vibration, thus several studies focused on developing a dynamical model of single or multiple stage planetary gears (Dhouib, et al., 2008). For instance, Lin and Parker (2002) developed a mathematical model of single-stage spur planetary gear and found out three modes such as rotational, translational and planet modes. Dhouib, et al., 2008 developed their own mathematical model of the planetary gearbox to investigate its dynamics. According to Ligata, Kahraman and Singh (2008) and Lynwander (1986) adding floating sun gear to planetary systems allows tolerating manufacturing errors to some extent, as well as reducing noise and vibration.

Moreover, Sun and Hu (2003) investigated nonlinear dynamics of planetary gear system by means of harmonic balance method and developed a lumped model which takes into consideration several clearances known to exist in a typical planetary gear system, such as gear backlash, time-dependent mesh stiffness due to static transmission error, excitation errors and shaft flexibility. Lumped modeling and finite element methods (FEM) are widely used to analyze gearing transmissions, but Wei, et al. (2017) proposed a new shafting element method and created a model to analyze coupling excitations in multistage planetary gearing

transmissions. The novel model provides a decent compromise between the accuracy of the lumped system and the complexity of FEM. According to the study, meshing frequency between different coupling components of planetary gears is crucial for dynamic excitations within the system and vibrational energy flows in both directions, independent of power flow direction. In the case of planetary gears with double-helical staggered teeth mesh, mesh vibrations are mostly dependent on stagger value (Sondkar & Kahraman, 2013). The occurrence of flaws within a planetary gear system due to premature failure of components influences the dynamic behavior significantly. For instance, Chen and Shao (2013) investigated a case of wind turbine planetary gear with a crack at the tooth root. They found out that sun gear tooth crack has a more severe impact on the dynamics of planetary gear comparing to planet gear tooth failure. In addition, Chen, Zhu, and Shao (2015) developed a method to detect a failure of a planetary gear based on the time-varying mesh stiffness graph and dynamic response. The results show that the flexibility of ring gear can reduce the amplitude of mesh stiffness response as well as mitigate the effect of tooth crack on the dynamic response. Ambarisha and Parker (2007) investigated the non-linear dynamics of spur planetary gears and developed two independent models: lumped and finite element based models. Both solutions display a coincidence between one another and able to predict dynamical excitations within the system. Also, there is a strong correlation between a number of planets in the system and a modal index of bending mode. In addition, manufacturing errors have a crucial effect on the dynamic response of planetary gears (Gu & Velez, 2013). Chaari et al., (2005) developed a plane model of a typical planetary gear and investigated the effects of manufacturing flaws such as profile error and eccentricity on dynamical response and overall performance. Analytical results showed low-frequency excitations for a properly manufactured model, whereas the model with manufacturing imperfections suffers from the abnormal dynamic response. For instance, adding the eccentricity led to the appearance of sidebands in the gear mesh signal, whilst the existence of profile error increased the amplitude of the signal. Zhou, Zhang, and Zhang (2016) who investigated the planetary gear system in shearer mechanisms reported that the influence of sun gear is largest to dynamical performance comparing with other gears. Moreover, statistically, they found out that the sun gear tooth width is the most crucial to the overall reliability among other structural and dimensional parameters.

Litvin, et al. (2002) proposed a new model of planetary gears with a crowned profile instead of traditional tooth geometry and replaced spur sun and ring gears with helical gears. As a result, the proposed model by authors displayed better performance comparing with the

conventional model, particularly enabling more even distribution of tooth load in planets and reduced transmission error (TE). Consequently, less vibration and noise. Mundo (2006) proposed a novel topology of a planetary gear set with non-circular gears that adopts the advantages of epicyclical gears. These types of mechanisms are able to provide a specific output torque curve, thus could possibly be used in applications where variable input/outputs are needed. Nutakor et al. (2017) developed an analytical model to estimate power losses in planetary gear systems, which are caused by non-uniform load distribution, the friction coefficient between components and oil viscosity. The method enables the calculation of a wide range of loss types for any velocity and temperature. According to the paper, mechanical losses within the system could be achieved by decreasing the gear module and increasing gear tooth pressure angle, with a compromise of increased noise. In addition, increasing a tooth width leads to a noticeable efficiency increase, while a gear-mesh loss could be reduced by adding teeth number.

Planetary gear sets have successful applications in renewable energy facilities as well. The most common example is wind turbines, where the planetary gear set is used to alter input velocity in order to ensure optimal working parameters of generators. However, according to the industry reports, 90% of wind generators have planetary gearboxes, and they tend to fail more often than other components. In the case of wind turbines, parameters such as alignment of gears and bearings, along with loads and stresses have a crucial influence on the overall reliability. Gear misalignment in planetary gear leads to time-varying mesh stiffness, increased loads in gears and bearing. Consequently, the fatigue life of the geared transmission diminishes drastically; dynamic response is affected negatively as well. In addition, undesirable clearances in carrier bearings caused by misalignment and excess wear could shorten the operational life of the planetary set and cause reliability issues (Crowther, Ramakrishnan, Zaidi, & Halse, 2011). Moreover, Guo, Keller, and Parker (2014) analyzed the effect of gravity on wind turbine planetary gearbox and created a lumped model, which includes gravitational forces, nonlinear mesh contact, time-dependent mesh stiffness and clearance between different gear components. According to the paper, the effect of gravity has a significant effect on the dynamic response of the gear and causes the tooth-wedging issue, which leads to the increased planet-bearing clearance, later to complete bearing failure. Apart from that, unusual clearance lowers a bearing stiffness and leads to a reduction of lowest resonant frequency, as a result, abnormal dynamic response. Another article dedicated to the planetary gear reliability issue was Nejad, Gao, and Moan (2014) who developed a mathematical model to estimate long-term fatigue effect on

planetary gears with wind turbine applications and evaluated its influence on the overall reliability. In the case of wind turbine planetary gearboxes, wind speeds close to the rated speed have the most negative effect on fatigue life. In addition, the authors claimed that in typical planetary gear sets, because of the higher cycle number and low teeth number, sun gear show the highest fatigue signs and tend to fail prematurely. Apart from the previous scholars, Gao, Xie, and Hu (2018) designed a new reliability model of planetary gears to predict their lifetime. While the existing reliability estimation method is purely static, the novel approach considers dynamic loads, which takes into account a random non-uniform load distribution case.

3.2. 3D Modelling

The topology of the novel planetary considers elimination of bearing interface between carrier and planets, and substitute these interface by geared connection. The main purpose of replacing the bearing interface by a more robust geared connection would make the gearbox more reliable. The circuit diagram is presented in Figure 3.1.

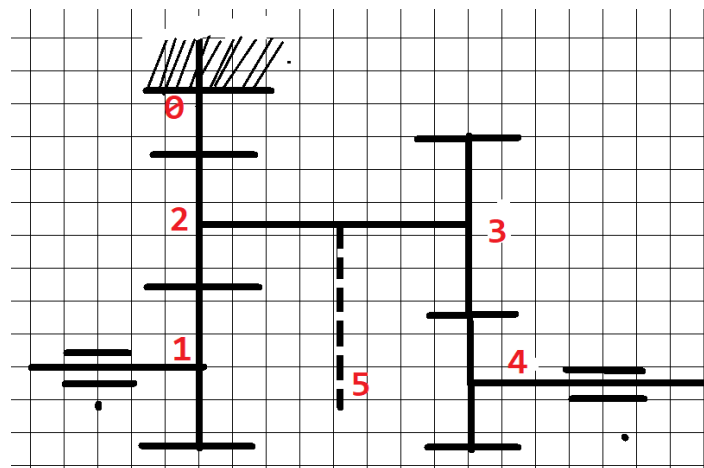
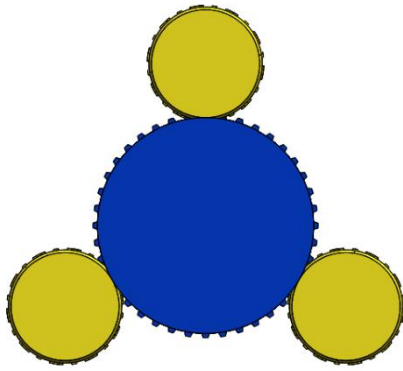


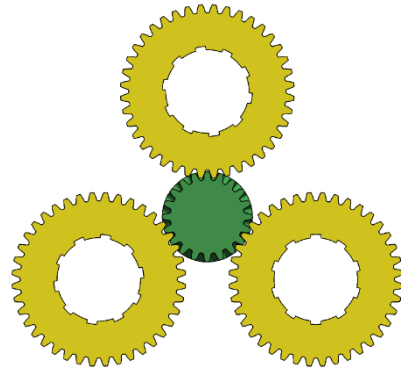
Figure 3. 1 *The circuit diagram of the proposed gear.*

(Here, 0 – ring gear (fixed), 1 – input shaft and sub gear, 2 – planets (primary planets), 3 – another set of spur gears rigidly connected with the planet (secondary planets), 4 – output gear and shaft)

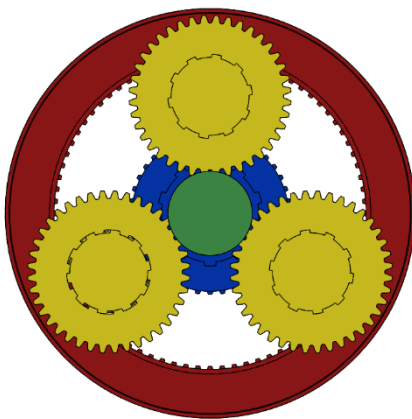
The main parts of the planetary gear were generated in the KissSoft platform. The main parts are ring gear, two sets of planets with different dimensions, sun gear as an input gear and output gear continued with the output shaft. Simply, a novel bearingless planetary gear with a floating carrier resembles an assembly of two planetary gear stages rigidly connected via planets' interfaces (Figure 3.2).



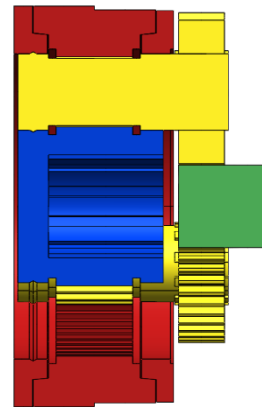
a) First planetary stage



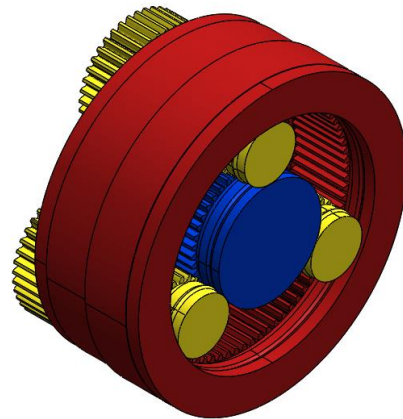
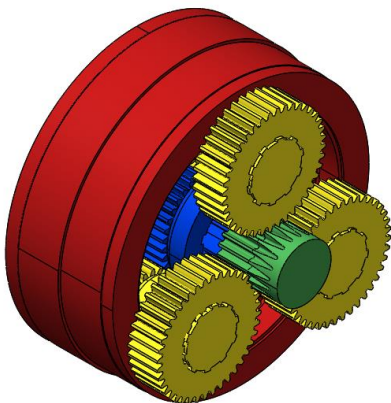
b) Second planetary stage



c) Front and back views



d) Cross-section view



e) Isometric views

Figure 3. 2 3D models of bearingless planetary gear with the floating carrier

In addition, to compensate alignment issues, a triangular raceway feature was added to the ring and input gears, whereas a similar triangular feature was introduced along with planets so that planets roll exactly along the grooves (Figure 3.3). The interfaces between raceways and gear define and maintain proper alignment of individual parts regarding one another.

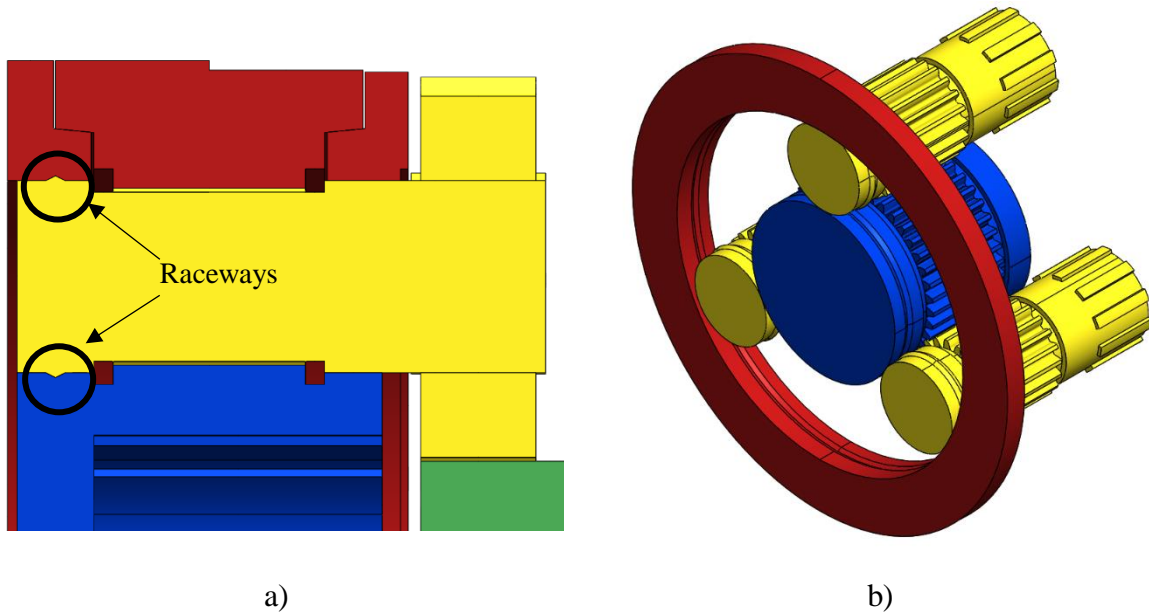


Figure 3. 3 Misalignment preventing raceways: a) cross-section view; b) location of triangular raceways in assembly

3.3. Numerical modeling

Numerical analysis of the proposed model of the planetary gearbox will be performed in ANSYS Mechanical by means of FEA in form of quasi-static simulation, while dynamical simulation will take place in MBD simulator RecurDyn. Both software has been being utilized for a long time to simulate powertrain systems, estimate loads and analyze kinematics.

Usually, gear contacts are the main concern when performing a numerical analysis of geared powertrains and require accurate modeling. Thus considering the complexity of the design with multiple gear contacts within the model, and taking into account limited computational power available, it was decided to simplify the model. Therefore, for the FEA in ANSYS, considering the symmetrical nature of the planetary gearbox, only one-third of the original design was examined during the quasi-static analysis. Conclusive models of the planetary gearbox used in FEA are given in Figure 3.4.

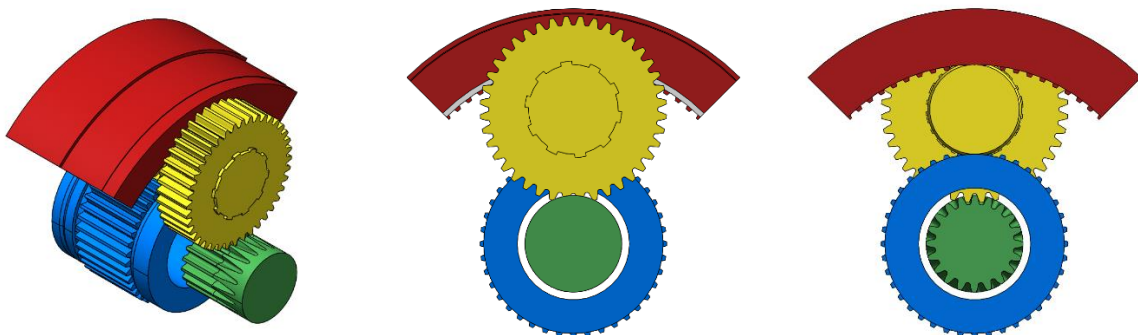


Figure 3.4 Simplified model of the planetary gear for quasi-static FEA

Boundary conditions for the quasi-static FEM analysis of the novel planetary gear are the following: input shaft was given a torque with a magnitude of 100 Nm and free to the rotational movement was given around its axis by means of cylindrical support. The first and second set of planetary gears were joined together by bonded contact characteristics. In addition, ring gear was fixed as well as the output shaft to resist the rotation. All gear interfaces within the model were given frictionless behavior to imitate the ideal case (Figure 3.5).

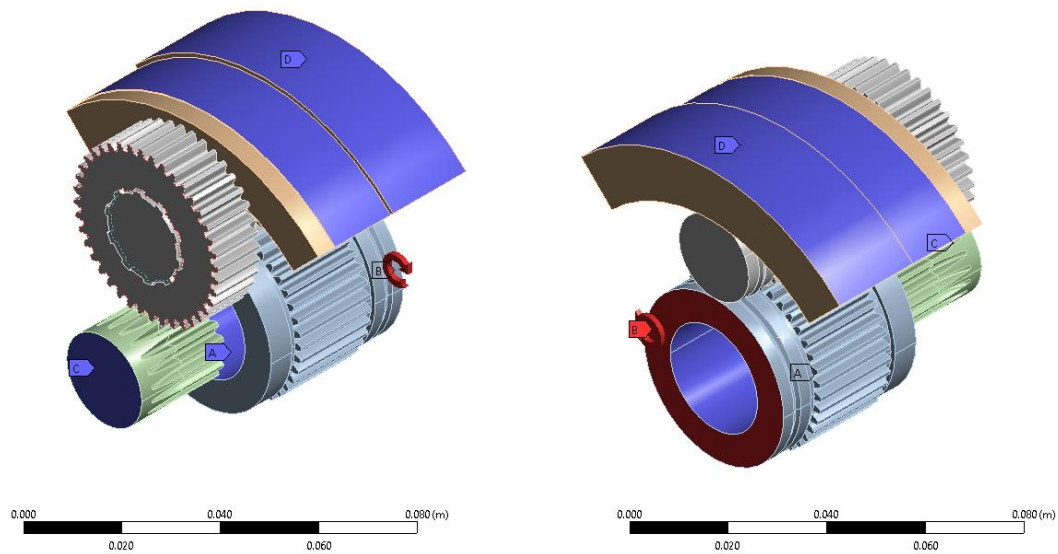
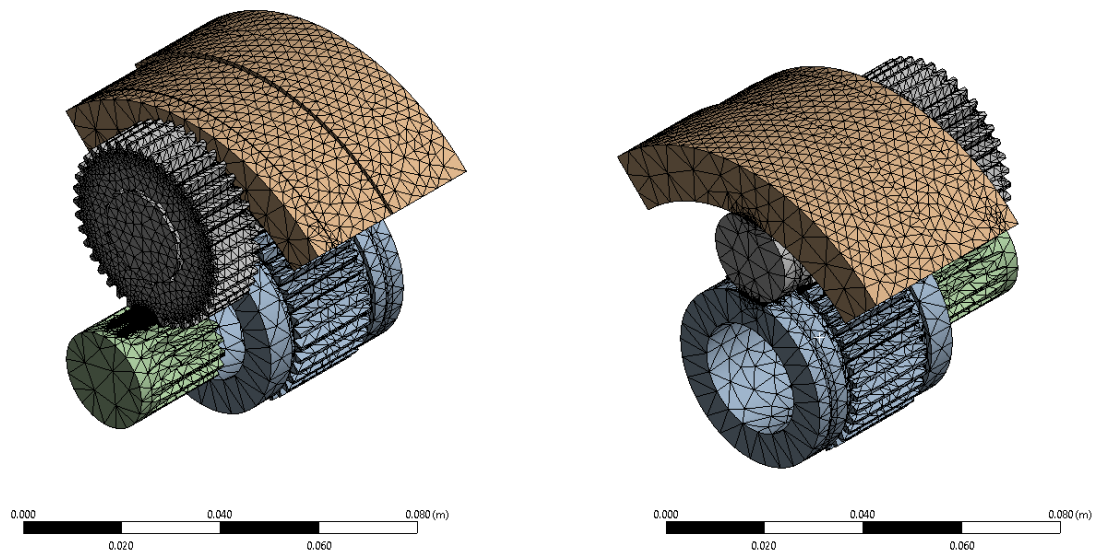
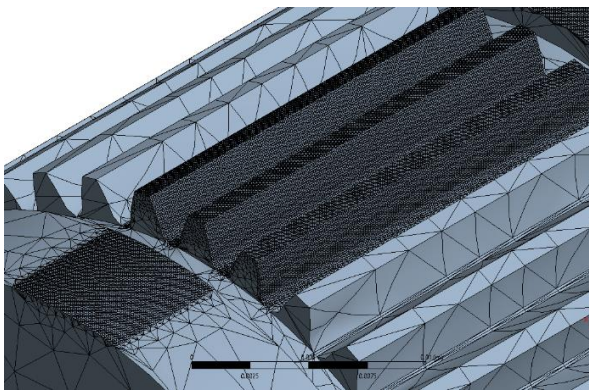


Figure 3.5 Boundary conditions for the planetary gear. Here, A) cylindrical support of input gear, B) moment (100 Nm), C) fixed support of output gear, D) fixed support of ring gear

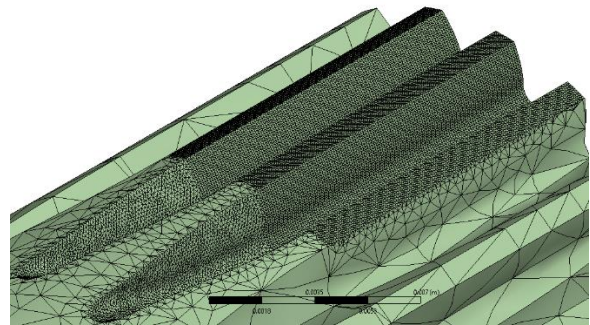
As in any FEA, discretization or meshing is vital for the analysis, and influence the accuracy of simulation significantly. Considering these facts, the main focus was on the gearing interfaces between individual spur gears of the planetary gearbox. Moreover, due to the limited capability of the workstation in terms of computational power and memory, it was impossible to discretize whole bodies. Thus mostly contacting gear surfaces were given the mesh with better quality. The final discretized model consists of more than 14000000 elements and around 23000000 nodes (Figure 3.6).



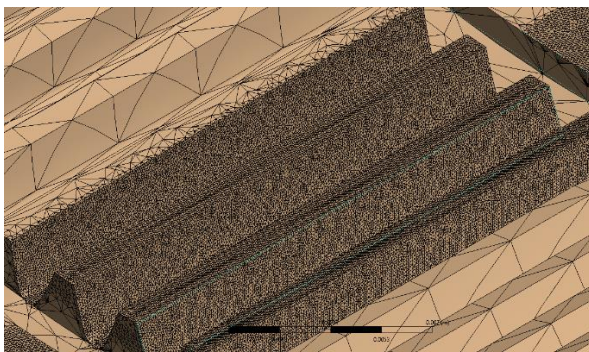
a) isometric views of the discretized model



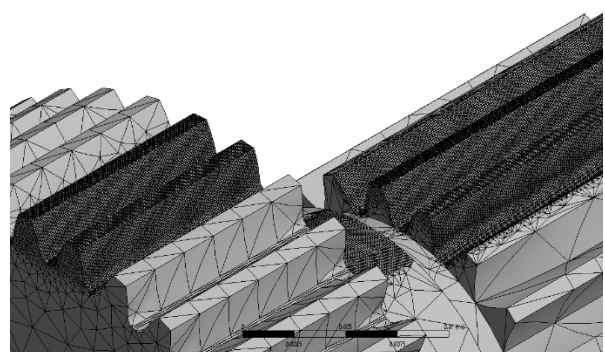
b) mesh elements of the input sun gear



c) mesh elements of the output gear



d) mesh elements of the ring gear



e) mesh elements of planets

Figure 3.6 Discretized model the planetary gear

Dynamical and kinematical simulations of the proposed design and benchmark system took place in multi-body dynamics (MBD) software called RecurDyn. The main purpose of the dynamical simulation is to observe the real-life behavior of the novel system and verify the initial hypothesis. Gear contacts define the overall behavior of the planetary gear set. Therefore,

appropriate modeling of the contact between gears possesses high importance. The software, in case of solid bodies, a pair contacting bodies are denoted as hitting and defense bodies. The interference between the hitting body and defense body is characterized as sphere-to-surface contact where the hitting body is replaced by multiple spheres, whereas the defense is discretized into multiple surfaces called patches. Thus, the software converts the initial solid-to-solid contact problem into surface-to-ball contact. In this case, the contact normal and friction forces are calculated as follows:

$$f_n = k\delta^{m1} + c \frac{\dot{\delta}}{|\dot{\delta}|} |\dot{\delta}|^{m2} \delta^{m3} \quad (3)$$

$$f_f = \mu |f_n| \quad (4)$$

These expressions, (3) and (4), fully define the contact problem in the MBD software. All gear tooth surfaces of individual gears such as primary, secondary planetary gears, ring gear, input and output gears are denoted as separate surfaces, since the surface-to-surface contact characteristics suit perfectly for this purpose, while body-to-body contact type is not capable to describe gear interfaces between individual bodies. These surface contacts are given frictionless characteristics, similar to the quasi-static simulations. In terms of boundary conditions, input shaft, as well as output shaft and the simulation environment are connected by a frictionless revolute joint. Moreover, the input shaft was given a rotational speed of 100 rads/sec, while the output shaft was given a 10 Nm torque to resist the rotation. Similar to the FEA simulation, the ring gear is fixed to the environment. Primary and secondary gears are joined together by fixed contact, at the same time they are in contact with input and output shaft, respectively, by means of surface-to-surface contacts. The full setup of the MBD analysis, including the synaptic network, is given in Figure 3.7.

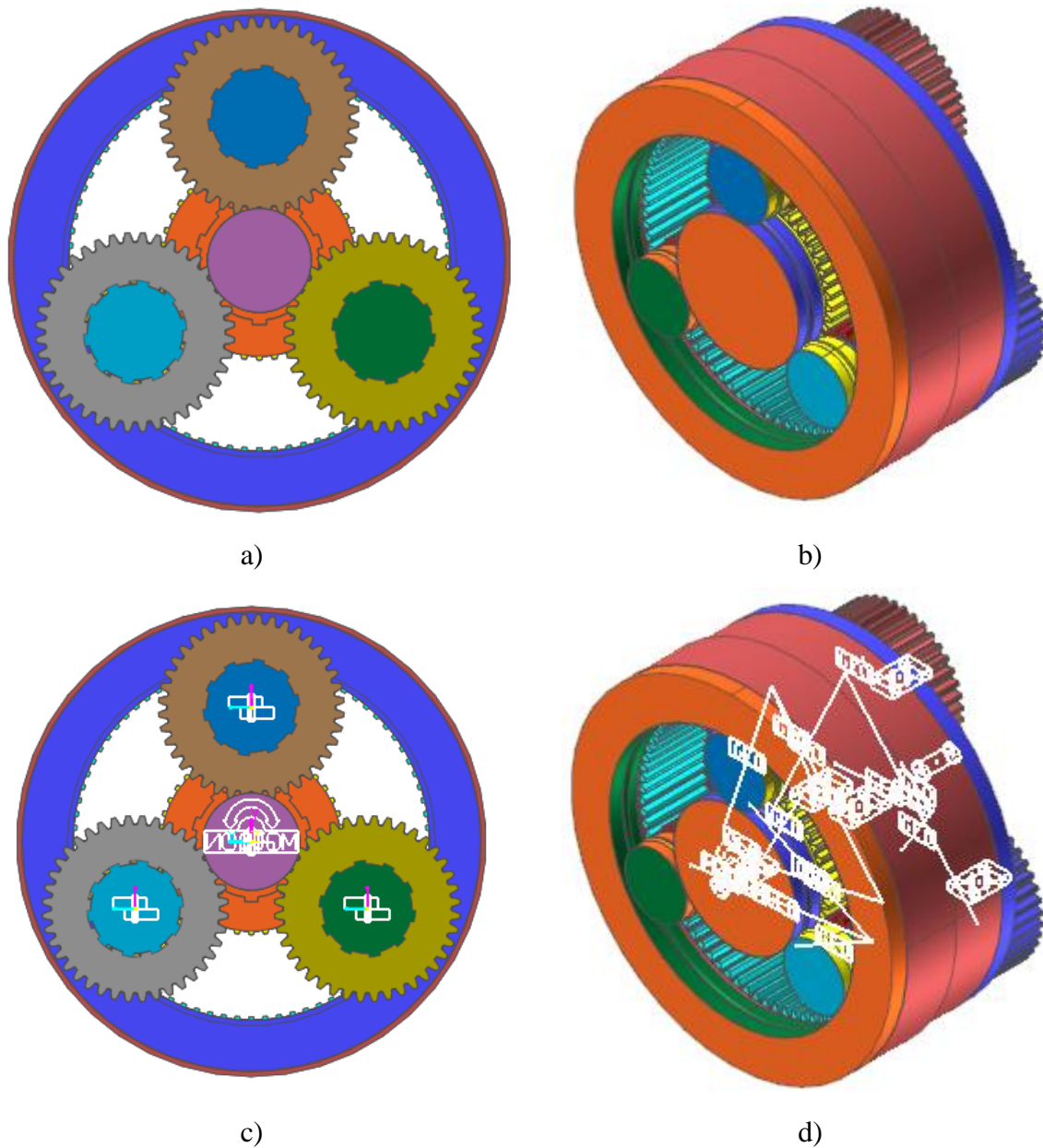
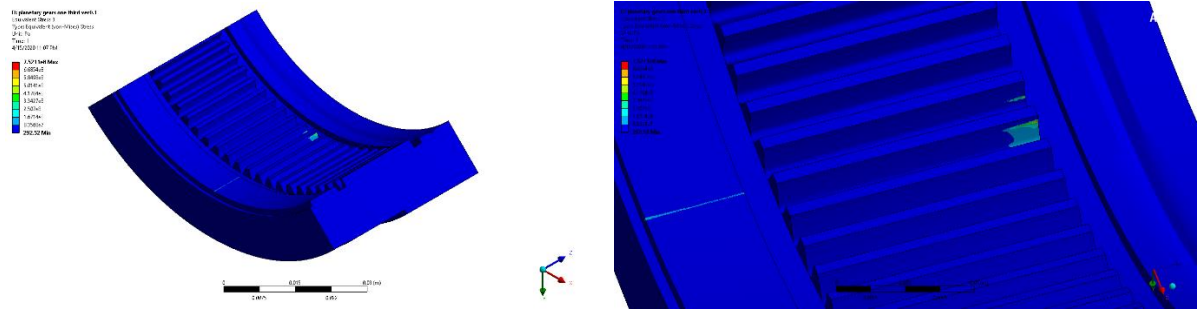


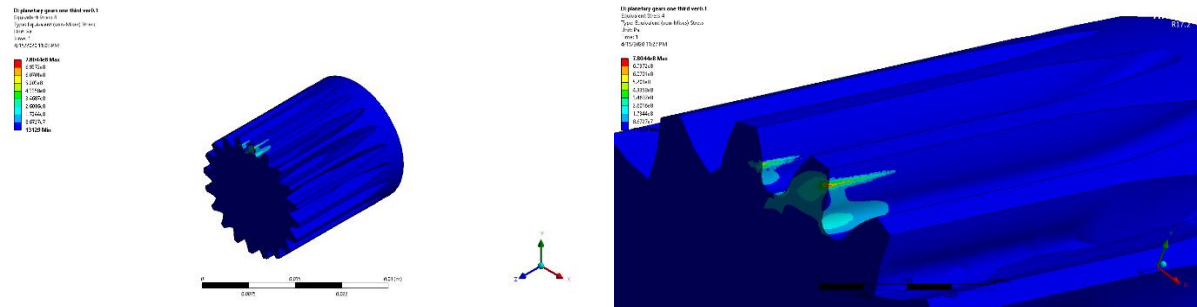
Figure 3.7 *MBD simulation setup for the bearingless planetary gearbox: a) front view of the model; b) isometric view; c) location of joints d) isometric view with synaptic network*

3.5. Results and discussion

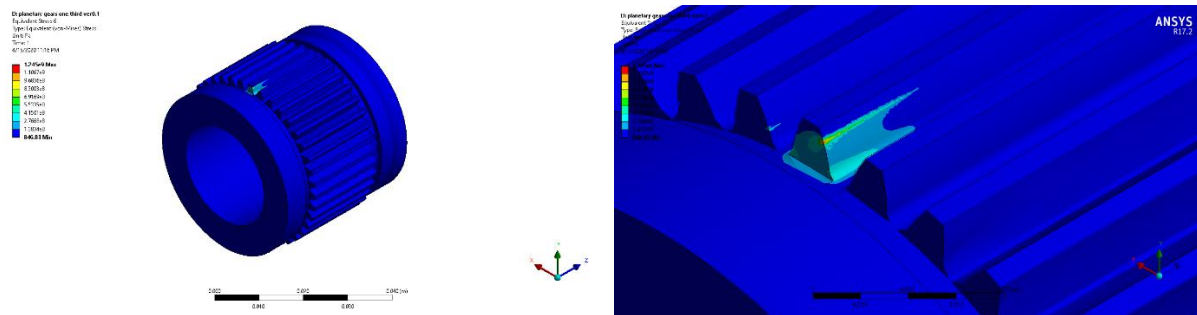
FEA of the bearingless planetary gear with a floating carrier demonstrated some interesting and unfavorable results. According to the numerical simulation stress distribution in gear, contacts are uneven along the primary contact lines. Extreme stress concentrations were observed on tooth edges and grooves, which is obviously undesired (Figure 3.8). This abnormal phenomenon indicates that the pair of connected primary and secondary planetary gears tends to turn sideways, which displays insufficiency of the proposed design to mitigate the misalignment issue which is inherent for planetary gear sets.



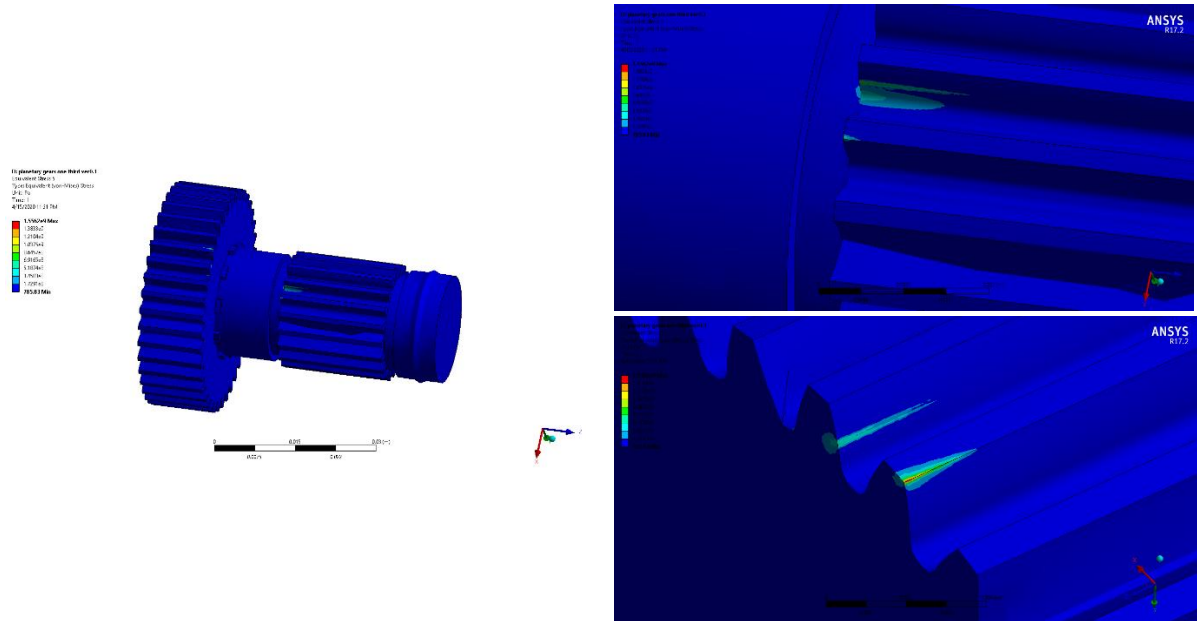
a) Stress distribution on the ring gear



b) Stress distribution on the output gear



c) Stress distribution on the input gear



d) Stress distribution on primary and secondary planets

Figure 3. 8 FEA results of the bearingless planetary gearbox with the floating carrier

In addition, these adverse state of the gearbox could be seen from the deformation plot (Figure 3.9). Under the applied loads, one end of the primary planetary gear shifts sideways causing extremely deflected state, which in turn, despite maximum deflection magnitude being just around 77 μm , leads to abnormal contact path, where the load is concentrated on the edge. This excessive deflection is probably caused by unbalanced forced developed in gear interfaces in bearingless planetary gear. Particularly forces are developed on interfaces between primary planetary gear and input shaft, as well as secondary planetary gear and output shaft. Unfortunately, the introduction of special grooves to compensate planet misalignment showed ineffectiveness against the issue. Operating under planets deflected condition obviously brings to premature failure of gear tooth due to irregular allocation of stresses. In addition, according to the previous misalignment part, these misaligned gears will generate noise and vibrations, which clearly leads to the complete destruction of the gearbox. Therefore, bearingless gearbox with floating carrier concepts requires thorough complete reevaluation and must undergo a design changing process where appropriate solutions could be found. These changes could be adding another set of grooves on the other side, or introducing a new set of planetary gears to compensate for the unbalanced forces. Unfortunately, current design topology was insufficient to solve the problem to meet the criteria of the robust, reliable and compact powertrain.

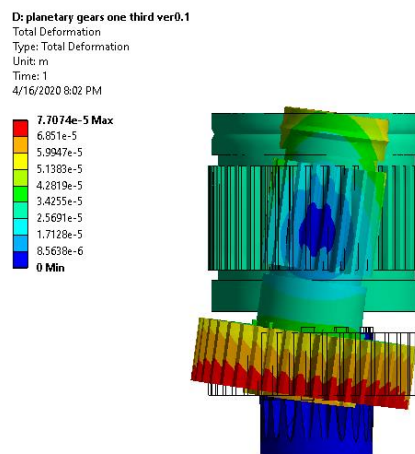


Figure 3. 9 Deformation results of the novel planetary gears (exaggerated, ring gear removed)

The main purpose of the MBD simulation was to demonstrate the workability and viability of the concept. The main reduction ratio of the model is estimated based on the rotational velocities of input and output. Velocity plots for input and output gears are given in Figure 3.10.

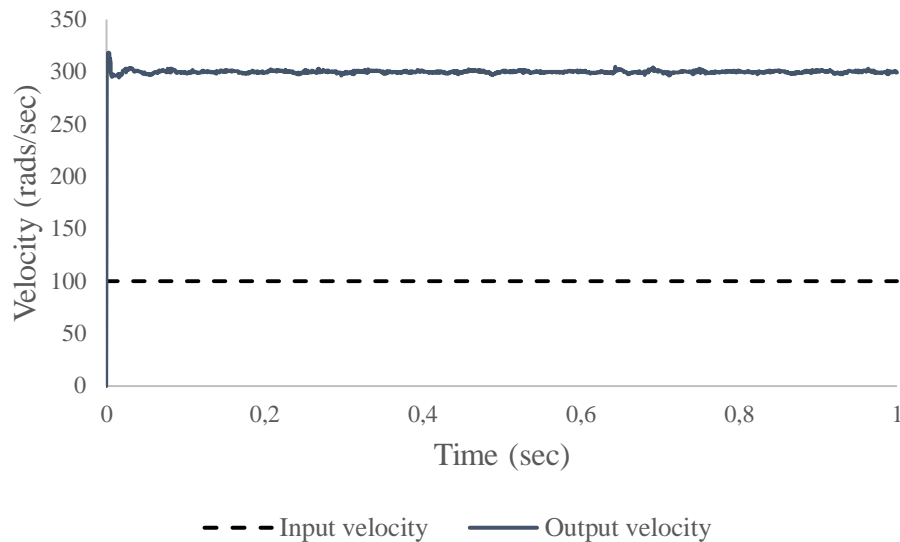


Figure 3. 10 Input and output velocity graphs for the bearingless planetary gearbox with the floating carrier

From the velocity graph, it's obvious that this particular design of the planetary gearbox has a reduction ratio of approximately 1:3. However, despite steady input velocity with the magnitude of 100 rads/sec, there is a slight fluctuation on the output side. These fluctuations could be caused by improper alignment of the planets, which was observed in the FEA results, where load distribution is not equal along the tooth contact lines. Thus, MBD simulation shows another unfavorable consequence of the misalignment of the planet such as non-uniform output velocity, which leads to another problem of torque ripple. To sum up, the topic of reliable and compact bearingless gearboxes with a floating carrier will be continued as a separate research project, where a more viable design concept will be considered.

Chapter 4 – Conclusion

Typical reliability issues of powertrains were considered in this thesis work, which is gear misalignment and common failures of planetary gearboxes. In the case of the misalignment, several promising solutions were proposed. One of the solutions is altering gear web to introduce flexibility and capability to reduce misalignment. Another solution came from the automotive industry in the form of a constant velocity ball joint or Rzeppa joint, which is designed to transfer torque between arbitrarily positioned shafts. Offered solutions were compared to conventional gear set which is the benchmark design and flank modified (crowned) design which is a wide-spread solution of gear misalignment. Benchmark model and crowned gears behaved as expected. There was a strong correlation between a maximum stress and

misalignment angle for the benchmark system, where stress valued increased rapidly when gears become misaligned. At the same time, crowned gears managed to prevent abnormal stress concentrations due to the elimination of sharp tooth corners, but decreased contact area between mating gears led to noticeable stress growth. Quasi-static FEA results showed the effectiveness of Rzeppa joint integrated design in terms of reducing stress concentrations along the primary contact line, with the trade-off being increased stress loads in ball-groove interfaces. However, this increase could be diminished by the application of high stress-resistant materials such as bearing ceramics. In addition, gears with kinematical joint were found to be insensitive to misalignment in terms of TE, which also proves the viability of the concept, and makes the most favorable design. Models with a compliant web demonstrated the decent capability of alleviating increased stress concentration in case of alignment error. Despite the effectiveness against the problem, due to the existence of thin elements, flexible web gears might suffer from buckling. Designing a bearingless planetary gearbox with a floating carrier showed some undesirable results. The main idea was to eliminate and replace carriers' bearing connection by robust gear tooth contact since the bearing often contributes to gearbox breakdown and improper alignment. Quasi-static and kinematical simulations revealed that a planetary gear with the proposed layout continues to undergo the same issues as regular gears. The addition of special grooves against misalignment failed either and showed ineffectiveness. Therefore, the topic of bearingless planetary gear with a floating carrier will find its continuation as a separate research project.

Bibliography

- Ambarisha, V. K., & Parker, R. G. (2007). Nonlinear dynamics of planetary gears using analytical and finite element models. *Journal of Sound and Vibration*, 302(3), 577–595. doi: 10.1016/j.jsv.2006.11.028
- Ameen, H. A. (2010). Effect of shaft misalignment on the stresses distribution of spur gears. *Engineering and Technology Journal*, 28(7), 1321-1339.
- Asi, O. (2006). Fatigue failure of a helical gear in a gearbox. *Engineering Failure Analysis*, 13(7), 1116–1125. doi: 10.1016/j.engfailanal.2005.07.020
- Amani, A., Spitas, V., & Spitas, C. (2015). Influence of centre distance deviation on the interference of a spur gear pair. *International Journal of Powertrains*, 4(4), 315-337.
- Amani, A., Spitas, C., & Spitas, V. (2017). Generalised non-dimensional multi-parametric involute spur gear design model considering manufacturability and geometrical compatibility. *Mechanism and Machine Theory*, 109, 250–277. doi: 10.1016/j.mechmachtheory.2016.11.012
- Barbato, G., Chiabert, P., D’Antonio, G., Maddis, M. D., Lombardi, F., & Ruffa, S. (2015). Method for automatic alignment recovery of a spur gear. *International Journal of Production Research*, 54(15), 4475-4486. doi:10.1080/00207543.2015.1064180
- Bergseth, E. B., & Björklund, S. B. (2010). Logarithmical Crowning for Spur Gears. *Journal of Mechanical Engineering*, 56(4), 239–244.
- Castillo, Jose M. del. 2002. “The Analytical Expression of the Efficiency of Planetary Gear Trains.” *Mechanism and Machine Theory* 37 (2): 197–214. [https://doi.org/10.1016/S0094-114X\(01\)00077-5](https://doi.org/10.1016/S0094-114X(01)00077-5).
- Chaari, F., Fakhfakh, T., Hbaieb, R., Louati, J., & Haddar, M. (2005). Influence of manufacturing errors on the dynamic behavior of planetary gears. *The International Journal of Advanced Manufacturing Technology*, 27(7-8), 738–746. doi: 10.1007/s00170-004-2240-2
- Chen, X., & Tang, J. (2011, August). Tooth contact analysis of spur face gear drives with alignment errors. In *Digital Manufacturing and Automation (ICDMA)*, 2011 Second International Conference on (pp. 1368-1371). IEEE.
- Chen, Z., & Shao, Y. (2013). Dynamic Features of a Planetary Gear System With Tooth Crack Under Different Sizes and Inclination Angles. *Journal of Vibration and Acoustics*, 135(3). doi: 10.1115/1.4023300

- Chen, Z., Zhu, Z., & Shao, Y. (2015). Fault feature analysis of planetary gear system with tooth root crack and flexible ring gear rim. *Engineering Failure Analysis*, 49, 92–103. doi: 10.1016/j.engfailanal.2014.12.014
- Cho, Sungtae, Kukhyun Ahn, and Jang Moo Lee. 2006. “Efficiency of the Planetary Gear Hybrid Powertrain.” *Proceedings of the Institution of Mechanical Engineers, Part D: Journal of Automobile Engineering* 220 (10): 1445–54. <https://doi.org/10.1243/09544070JAUTO176>.
- Choy, F. K., Jia, W., & Wu, R. (2009). Identification of bearing and gear tooth damage in a transmission system. *Tribology Transactions*, 52(3), 303-309.
- Crowther, A., Ramakrishnan, V., Zaidi, N. A., & Halse, C. (2011). Sources of time-varying contact stress and misalignments in wind turbine planetary sets. *Wind Energy*, 14(5), 637–651. doi: 10.1002/we.447
- Dhouib, S., Hbaieb, R., Chaari, F., Abbes, M. S., Fakhfakh, T., & Haddar, M. (2008). Free vibration characteristics of compound planetary gear train sets. *Proceedings of the Institution of Mechanical Engineers, Part C: Journal of Mechanical Engineering Science*, 222(8), 1389–1401. doi: 10.1243/09544062jmes870
- Eng, J., & Patil, S. (2018). Frictional stress analysis of spur gear with misalignments. *Journal Of Mechanical Engineering And Sciences*, 12 (2), 3566-3580. doi:10.15282/jmes.12.2.2018.4.316
- Gao, P., Xie, L., & Hu, W. (2018). Reliability and Random Lifetime Models of Planetary Gear Systems. *Shock and Vibration*, 2018, 1–12. doi: 10.1155/2018/9106404
- Glodez, S. (1998). Experimental results of the fatigue crack growth in a gear tooth root. *International Journal of Fatigue*, 20 (9), 669-675. doi:10.1016/s0142-1123(98)00040-1
- Gu, X., & Velex, P. (2013). On the dynamic simulation of eccentricity errors in planetary gears. *Mechanism and Machine Theory*, 61, 14–29. doi: 10.1016/j.mechmachtheory.2012.10.003
- Guo, Y., Keller, J., & Lacava, W. (2014). Planetary gear load sharing of wind turbine drivetrains subjected to non-torque loads. *Wind Energy*, 18(4), 757–768. doi: 10.1002/we.1731
- Guo, Y., Keller, J., & Parker, R. G. (2014). Nonlinear dynamics and stability of wind turbine planetary gear sets under gravity effects. *European Journal of Mechanics - A/Solids*, 47, 45–57. doi: 10.1016/j.euromechsol.2014.02.013

Haigh, J., & Fawcett, J. N. (2003). Effects of misalignment on load distribution in large face-width helical gears. *Proceedings of the Institution of Mechanical Engineers, Part K: Journal of Multi-body Dynamics*, 217(2), 93-98.

Hotait, M. A., Talbot, D., & Kahraman, A. (2007, January). An investigation of the influence of shaft misalignments on bending stresses of helical gear with lead crown. In ASME 2007 International Design Engineering Technical Conferences and Computers and Information in Engineering Conference (pp. 929-937). American Society of Mechanical Engineers.

Hu, Z., & Mao, K. (2017). An investigation of misalignment effects on the performance of acetal gears. *Tribology International*, 116, 394-402. doi:10.1016/j.triboint.2017.07.029

Jammal, A., Wang, H., & Rong, Y. (2015). Spur Gears Static and Dynamic Meshing Simulation and Tooth Stress Calculation. In MATEC Web of Conferences (Vol. 26, p. 03001). EDP Sciences.

Kao, Wei-Pu, Chang-Chia Hsieh, and Jyh-Jone Lee. 2015. "Computer-Aided Kinematic Error Analysis of a Two-Stage Cycloidal Drive." The 14th IFToMM World Congress, October. <https://doi.org/10.6567/IFTToMM.14TH.WC.OS6.013>.

Kahraman, A., Kharazi, A., & Umrani, M. (2003). A deformable body dynamic analysis of planetary gears with thin rims. *Journal of Sound and Vibration*, 262(3), 752–768. doi: 10.1016/s0022-460x(03)00122-6

Kumar, P., Hirani, H., & Agrawal, A. K. (2019). Effect of gear misalignment on contact area: Theoretical and experimental studies. *Measurement*, 132, 359-368. doi:10.1016/j.measurement.2018.09.070

Li, S. (2012). Contact stress and root stress analyses of thin-rimmed spur gears with inclined webs. *Journal of Mechanical Design*, 134(5), 051001.

Li, S. (2015). An investigation on the influence of misalignment on micro-pitting of a spur gear pair. *Tribology Letters*, 60(3), 35.

Li, M., Xie, L., & Ding, L. (2017). Load sharing analysis and reliability prediction for planetary gear train of helicopter. *Mechanism and Machine Theory*, 115, 97–113. doi: 10.1016/j.mechmachtheory.2017.05.001

Lin, J., & Parker, R. (2002). Planetary Gear Parametric Instability Caused By Mesh Stiffness Variation. *Journal of Sound and Vibration*, 249(1), 129–145. doi: 10.1006/jsvi.2001.3848

Litvin, F. L., Vecchiato, D., Demenego, A., Karedes, E., Hansen, B., & Handschuh, R. (2002). Design of One Stage Planetary Gear Train With Improved Conditions of Load Distribution and Reduced Transmission Errors. *Journal of Mechanical Design*, 124(4), 745–752. doi: 10.1115/1.1515797

Liu, Jinming, and Huei Peng. 2010. “A Systematic Design Approach for Two Planetary Gear Split Hybrid Vehicles.” *Vehicle System Dynamics* 48 (11): 1395–1412. <https://doi.org/10.1080/00423114.2010.512634>.

Mackic, T., M. Blagojevic, Z. Babic, and N. Kostic. 2013. “Influence of Design Parameters on Cyclo Drive Efficiency.” *Journal of the Balkan Tribological Association* 19 (4): 497–597.

Manriota, Giacomo, and Ettore Pennestri. 2003. “Theoretical and Experimental Efficiency Analysis of Multi-Degrees-of-Freedom Epicyclic Gear Trains.” *Multibody System Dynamics*, 9 (4): 389–408. <https://doi.org/10.1023/A:1023319515306>.

Mao, K. (2007). Gear tooth contact analysis and its application in the reduction of fatigue wear. *Wear*, 262(11-12), 1281-1288.

Mundo, D. (2006). Geometric design of a planetary gear train with non-circular gears. *Mechanism and Machine Theory*, 41(4), 456–472. doi: 10.1016/j.mechmachtheory.2005.06.003

Neha, G., & Shunmugam, M. (2017). Effect of shaft misalignment and mitigation through crowning in spur gear transmission. *International Journal of Computer Aided Engineering and Technology*, 9(4), 385. doi:10.1504/ijcaet.2017.086919

Nejad, A. R., Gao, Z., & Moan, T. (2014). On long-term fatigue damage and reliability analysis of gears under wind loads in offshore wind turbine drivetrains. *International Journal of Fatigue*, 61, 116–128. doi: 10.1016/j.ijfatigue.2013.11.023

Nutakor, C., Kłodowski, A., Sopenan, J., Mikkola, A., & Pedrero, J. I. (2017). Planetary gear sets power loss modeling: Application to wind turbines. *Tribology International*, 105, 42–54. doi: 10.1016/j.triboint.2016.09.029

Park, J., Ha, J. M., Oh, H., Youn, B. D., Choi, J.-H., & Kim, N. H. (2016). Model-Based Fault Diagnosis of a Planetary Gear: A Novel Approach Using Transmission Error. *IEEE Transactions on Reliability*, 65(4), 1830–1841. doi: 10.1109/tr.2016.2590997

Pennestrì, E., and F. Freudenstein. 1993. "The Mechanical Efficiency of Epicyclic Gear Trains." *Journal of Mechanical Design* 115 (3): 645–51. <https://doi.org/10.1115/1.2919239>.

Pennestrì, Ettore, and Pier Paolo Valentini. 2003. "A Review of Formulas for the Mechanical Efficiency Analysis of Two Degrees-of-Freedom Epicyclic Gear Trains." *Journal of Mechanical Design* 125 (3): 602–8. <https://doi.org/10.1115/1.1587157>.

Pennestrì, E., & Valentini, P. P. (2008). Kinematic design and multi-body analysis of Rzeppa pilot-lever joint. *Proceedings of the Institution of Mechanical Engineers, Part K: Journal of Multi-body Dynamics*, 222(2), 135-142.

Randl, Chad. 2008. *Revolving Architecture: A History of Buildings That Rotate, Swivel, and Pivot*. Princeton Architectural Press.

Rzeppa, A. H. (1936). U.S. Patent No. 2,046,584. Washington, DC: U.S. Patent and Trademark Office.

Pop, N., & Crețu, S. (2017). Tooth contact analysis of spur gears. Part 2-Analysis of modified gears. In *MATEC Web of Conferences* (Vol. 112, p. 07016). EDP Sciences.

Royston, T. J., & Basdogan, I. (1998). Vibration transmission through self-aligning (spherical) rolling element bearings: theory and experiment. *Journal of Sound and Vibration*, 215(5), 997-1014.

Saxena, A., Parey, A., & Chouksey, M. (2015). Effect of shaft misalignment and friction force on time varying mesh stiffness of spur gear pair. *Engineering Failure Analysis*, 49, 79-91. doi:10.1016/j.engfailanal.2014.12.020

Savage, M., Paridon, C. A., & Coy, J. J. (1983). Reliability model for planetary gear trains.

Sensingier, J. W., and J. H. Lipsey. 2012. "Cycloid vs. Harmonic Drives for Use in High Ratio, Single Stage Robotic Transmissions." In 2012 IEEE International Conference on Robotics and Automation, 4130–35. <https://doi.org/10.1109/ICRA.2012.6224739>.

Sensingier, Jonathon W. 2013. "Efficiency of High-Sensitivity Gear Trains, Such as Cycloid Drives." *Journal of Mechanical Design* 135 (7): 071006-071006–9. <https://doi.org/10.1115/1.4024370>.

Seol, I. H., & Kim, D. H. (1998). The kinematic and dynamic analysis of crowned spur gear drive. *Computer methods in applied mechanics and engineering*, 167(1-2), 109-118.

- Simionescu, P. A. 1998. "A Unified Approach to the Assembly Condition of Epicyclic Gears." *Journal of Mechanical Design* 120 (3): 448–52. <https://doi.org/10.1115/1.2829172>.
- Shubham, B., & Nimish, A. (2016). Static and dynamic analysis of spur gear. *International Journal of Mechanical Engineering and Technology (IJMET)*, 7(4), 8-21.
- Sánchez, M. B., Pleguezuelos, M., & Pedrero, J. I. (2016). Calculation of tooth bending strength and surface durability of internal spur gear drives. *Mechanism and Machine Theory*, 95, 102-113.
- Spitas, C., & Spitas, V. (2006). Calculation of overloads induced by indexing errors in spur gearboxes using multi-degree-of-freedom dynamical simulation. *Proceedings of the Institution of Mechanical Engineers, Part K: Journal of Multi-body Dynamics*, 220(4), 273-282.
- Sondkar, P., & Kahraman, A. (2013). A dynamic model of a double-helical planetary gear set. *Mechanism and Machine Theory*, 70, 157–174. doi: 10.1016/j.mechmachtheory.2013.07.005
- Sun, Tao, and HaiYan Hu. 2003. "Nonlinear Dynamics of a Planetary Gear System with Multiple Clearances." *Mechanism and Machine Theory* 38 (12): 1371–90. [https://doi.org/10.1016/S0094-114X\(03\)00093-4](https://doi.org/10.1016/S0094-114X(03)00093-4).
- Tsai, Mi-Ching, Cheng-Chi Huang, and Bor-Jeng Lin. 2010. "Kinematic Analysis of Planetary Gear Systems Using Block Diagrams." *Journal of Mechanical Design* 132 (6): 065001-065001–10. <https://doi.org/10.1115/1.4001598>.
- Wei, J., Zhang, A., Qin, D., Lim, T. C., Shu, R., Lin, X., & Meng, F. (2017). A coupling dynamics analysis method for a multistage planetary gear system. *Mechanism and Machine Theory*, 110, 27–49. doi: 10.1016/j.mechmachtheory.2016.12.007
- Ye, S., & Tsai, S. (2016). A computerized method for loaded tooth contact analysis of high-contact-ratio spur gears with or without flank modification considering tip corner contact and shaft misalignment. *Mechanism and Machine Theory*, 97, 190-214. doi:10.1016/j.mechmachtheory.2015.11.008
- Young, F. (2010, March/April). Crowning: a cheap fix for noise reduction and misalignment problems. *Gear Technology*, 12-13.

Yuksel, C., and A. Kahraman. 2004. "Dynamic Tooth Loads of Planetary Gear Sets Having Tooth Profile Wear." *Mechanism and Machine Theory* 39 (7): 695–715. <https://doi.org/10.1016/j.mechmachtheory.2004.03.001>.

Zhou, D., Zhang, X., & Zhang, Y. (2016). Dynamic reliability analysis for planetary gear system in shearer mechanisms. *Mechanism and Machine Theory*, 105, 244–259. doi: 10.1016/j.mechmachtheory.2016.07.007